Microcrystal electron diffraction theory and application

Cryo-EM Course at the Laboratory for BioMolecular Structure (LBMS)

6.23.2023

Max T.B. Clabbers
Department of Biological Chemistry
David Geffen School of Medicine
University of California, Los Angeles
clabbers@ucla.edu

UCLA

David Geffen School of Medicine

Typical workflow in macromolecular structure determination using electron crystallography

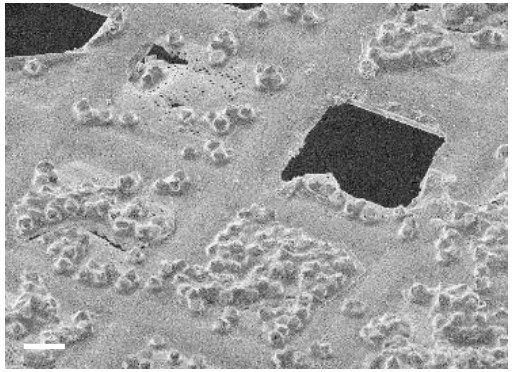

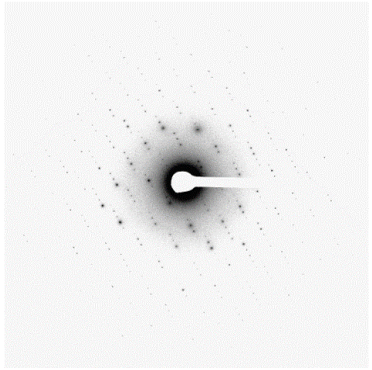

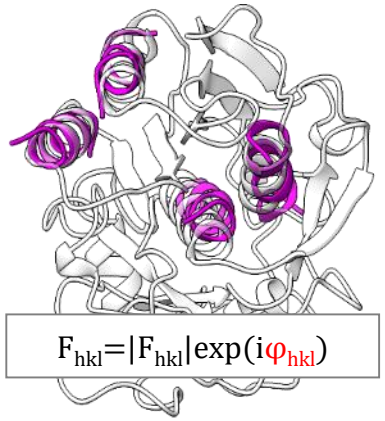

Crystallization | Vitrification | FIB/SEM | MicroED | Data processing | Phasing | Model building & refinement

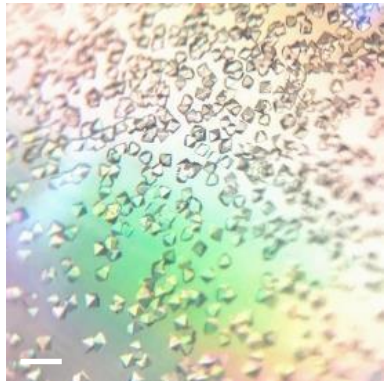

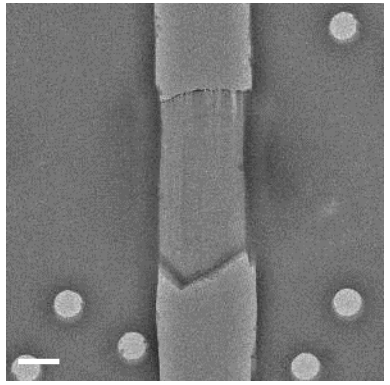

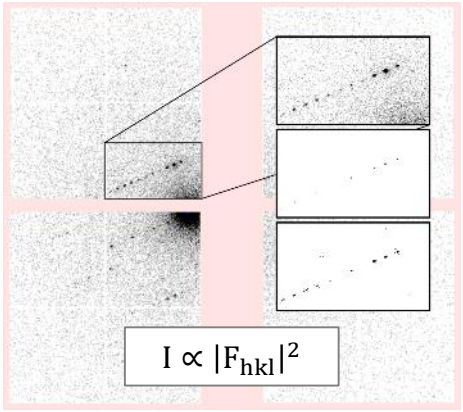

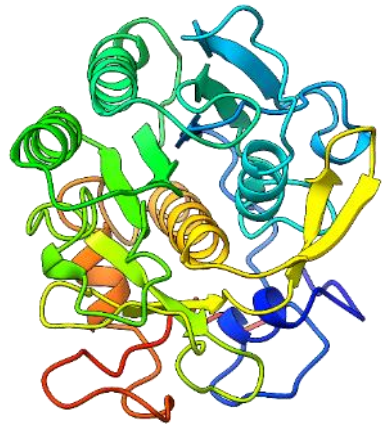

Electrons are several orders of magnitude less damaging than X-rays

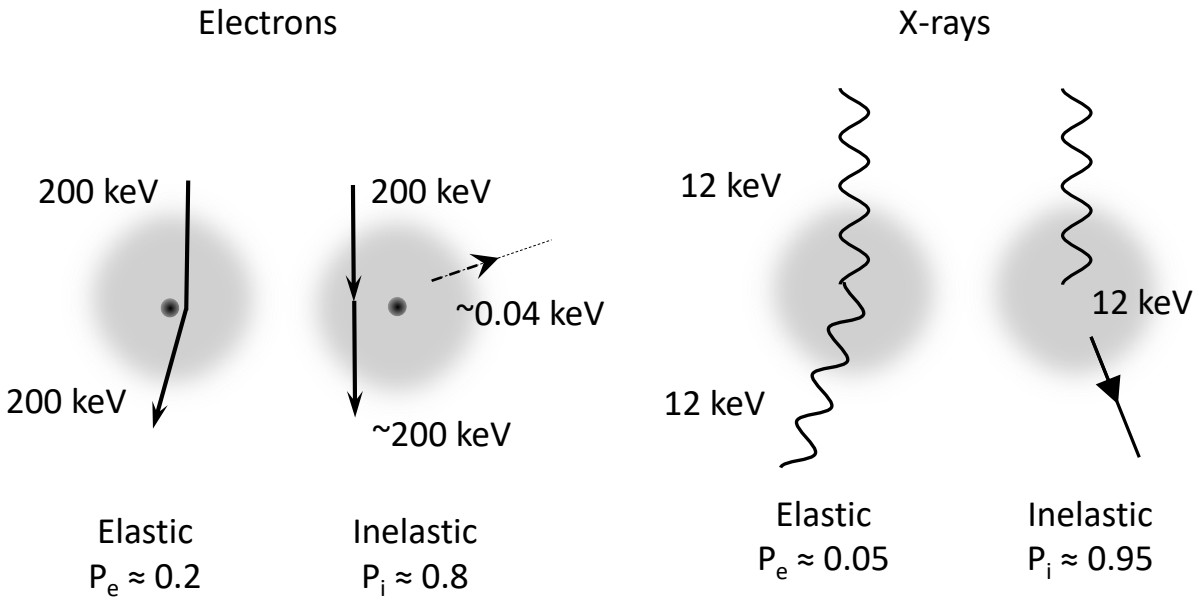

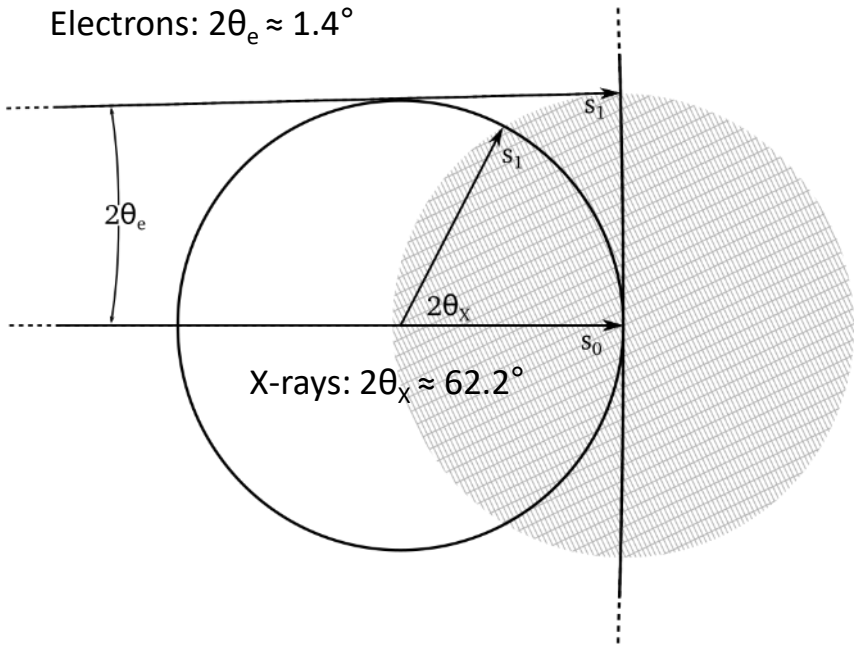

- ❑ Electrons are scattered by the electrostatic potential
- ❑ 10^3 times less energy per useful diffracted quantum
- ❑ Increased contrast for resolving hydrogen atoms
- ❑ Potential to visualize charge distribution of atoms

- ❑ Diffraction geometry and Ewald construction
- ❑ The Ewald sphere is virtually flat
- ❑ Generally do not observe higher order Laue zones
- ❑ Friedel pairs can be measured on the same frame

Microcrystalline samples suitable for electron diffraction structure determination

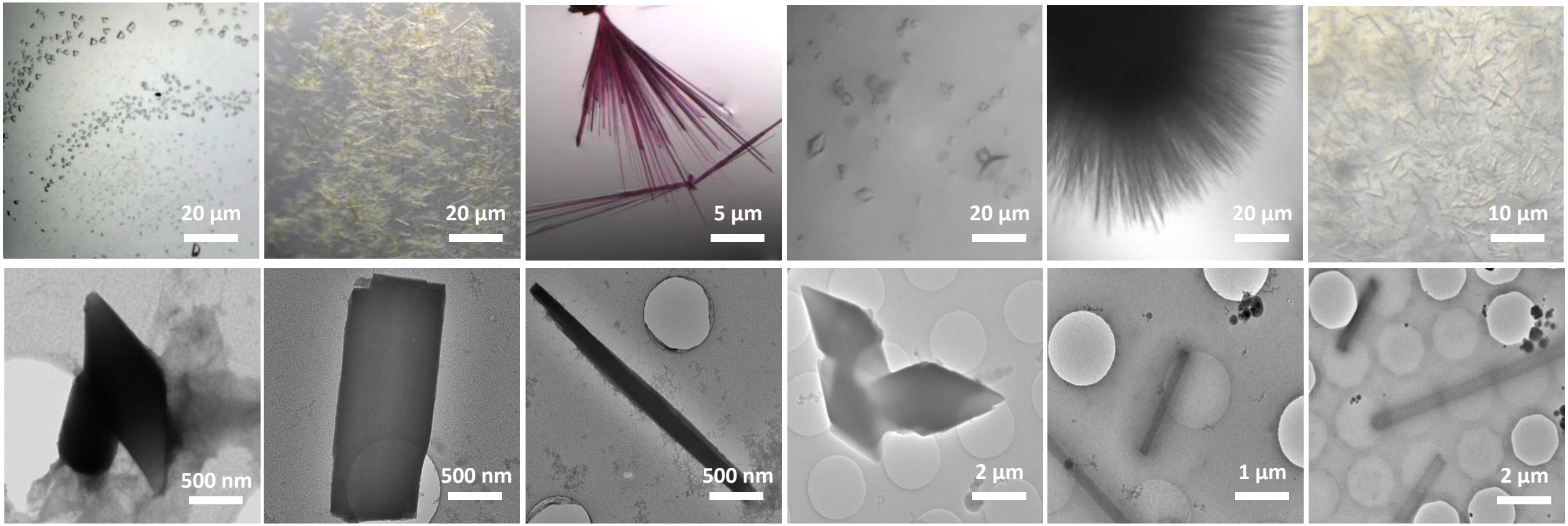

MyD88 TIR domain higher order assembly interactions revealed by MicroED

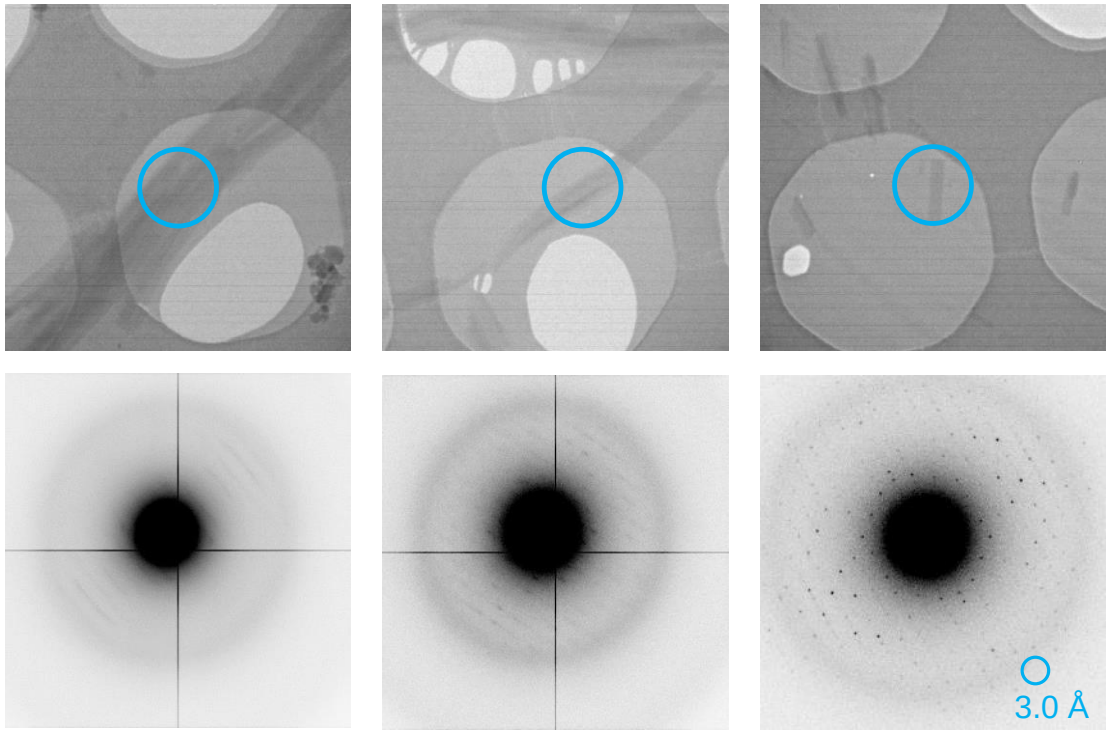

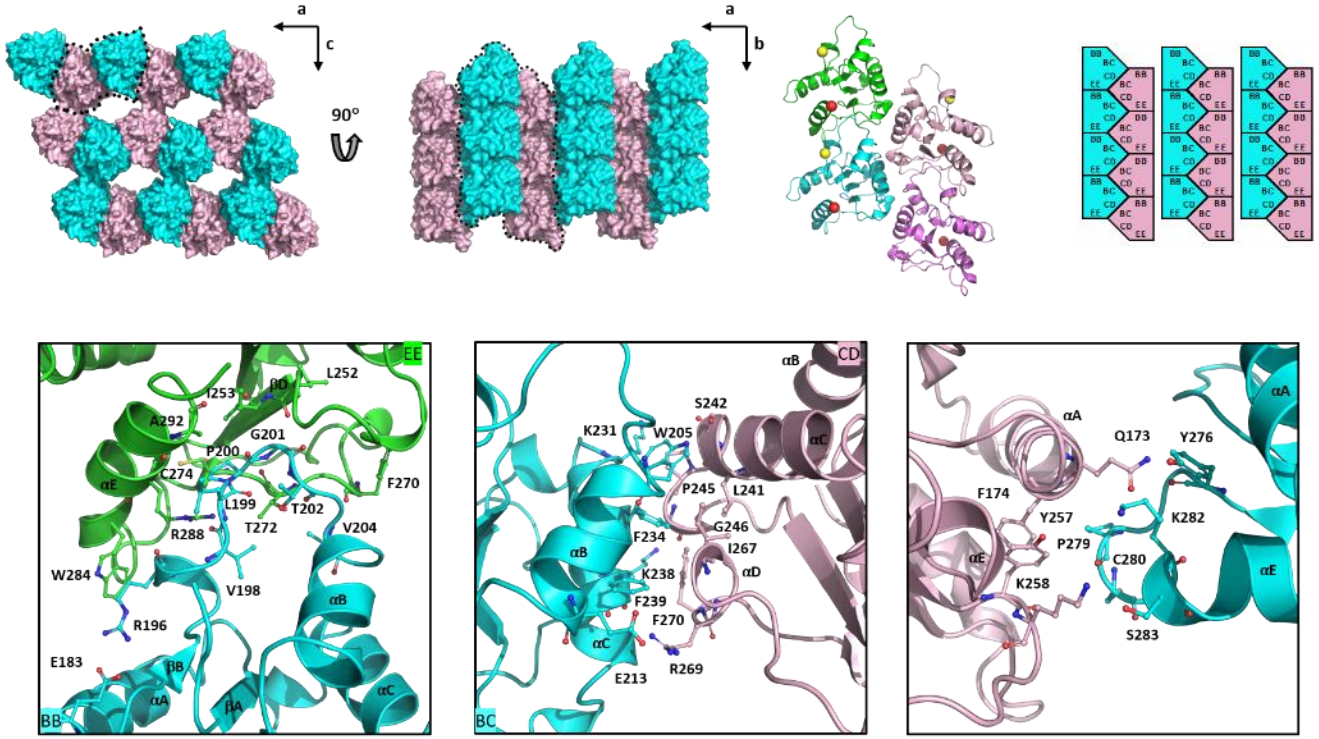

Clabbers *et al., Nat. Commun.* 12, 2578 (2021)

Solving the structure of a previously unknown R2lox metalloenzyme by MicroED

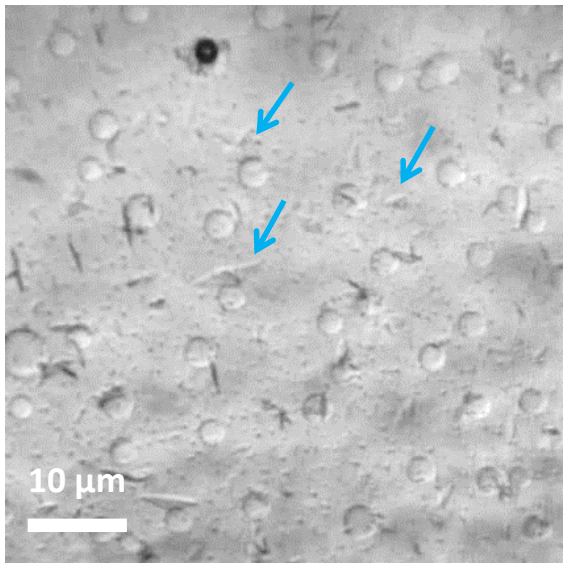

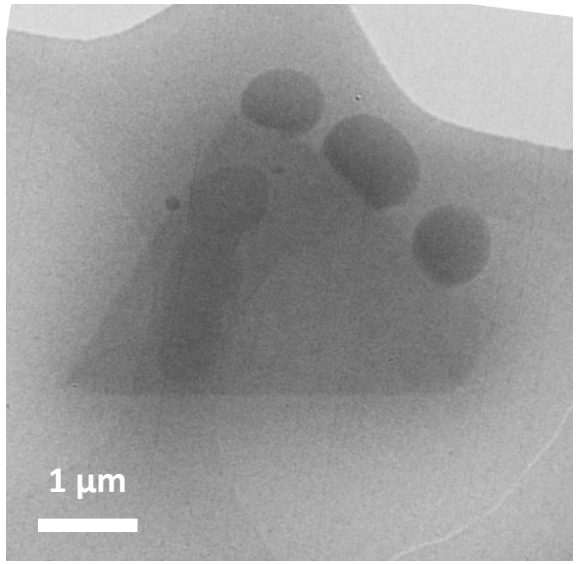

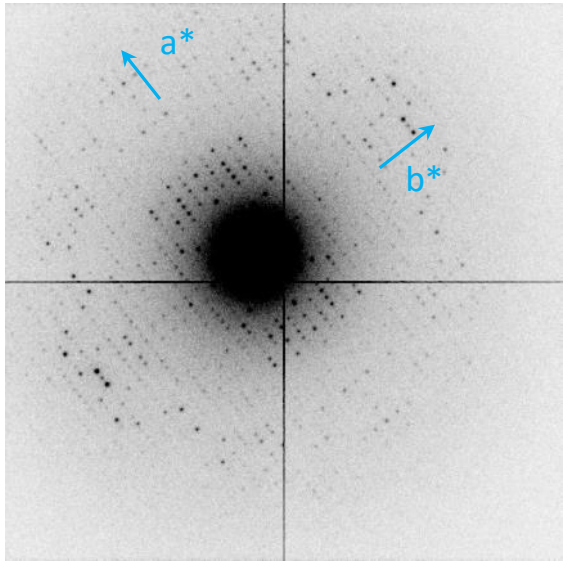

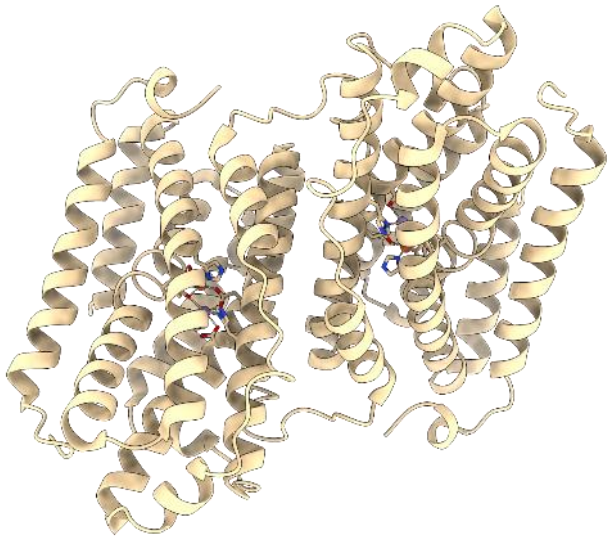

Microcrystals grown in 44% (v/v) PEG 400 ⟶ Highly viscous

Xu, Lebrette, Clabbers *et al., Sci. Adv.* 5, eaax4621 (2019)

Fragmentation of macrocrystals to smaller microcrystalline fragments

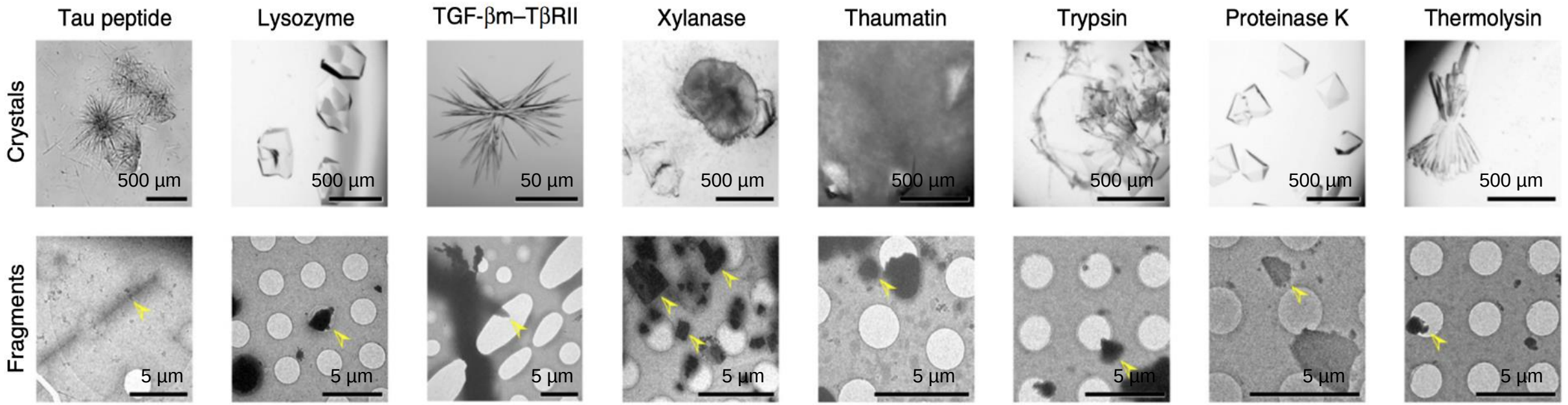

de la Cruz *et al.*, *Nat. Methods* 14, 399-402 (2017)

Preparing thin crystalline lamellae using focused ion beam (FIB) milling

SEM

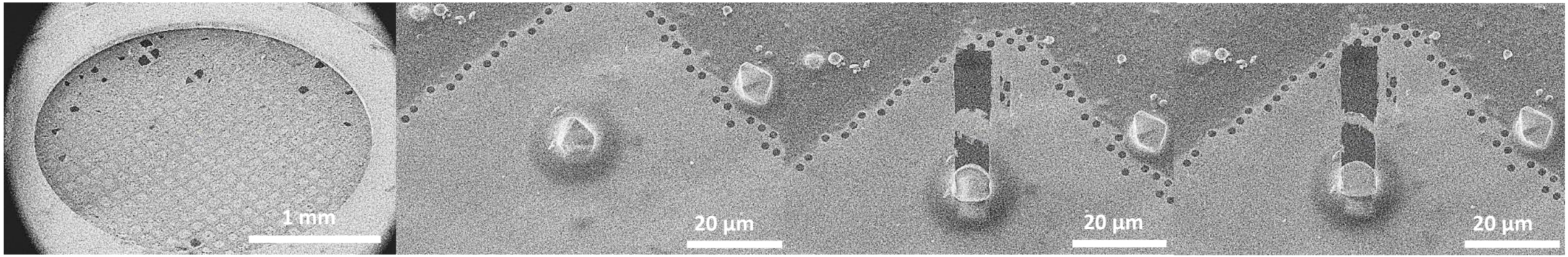

FIB

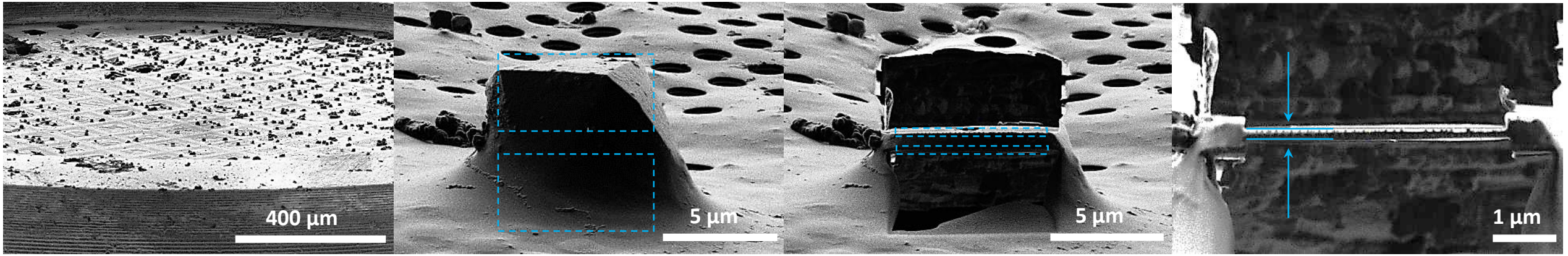

Benchmarking the ideal sample thickness for cryo-EM experiments

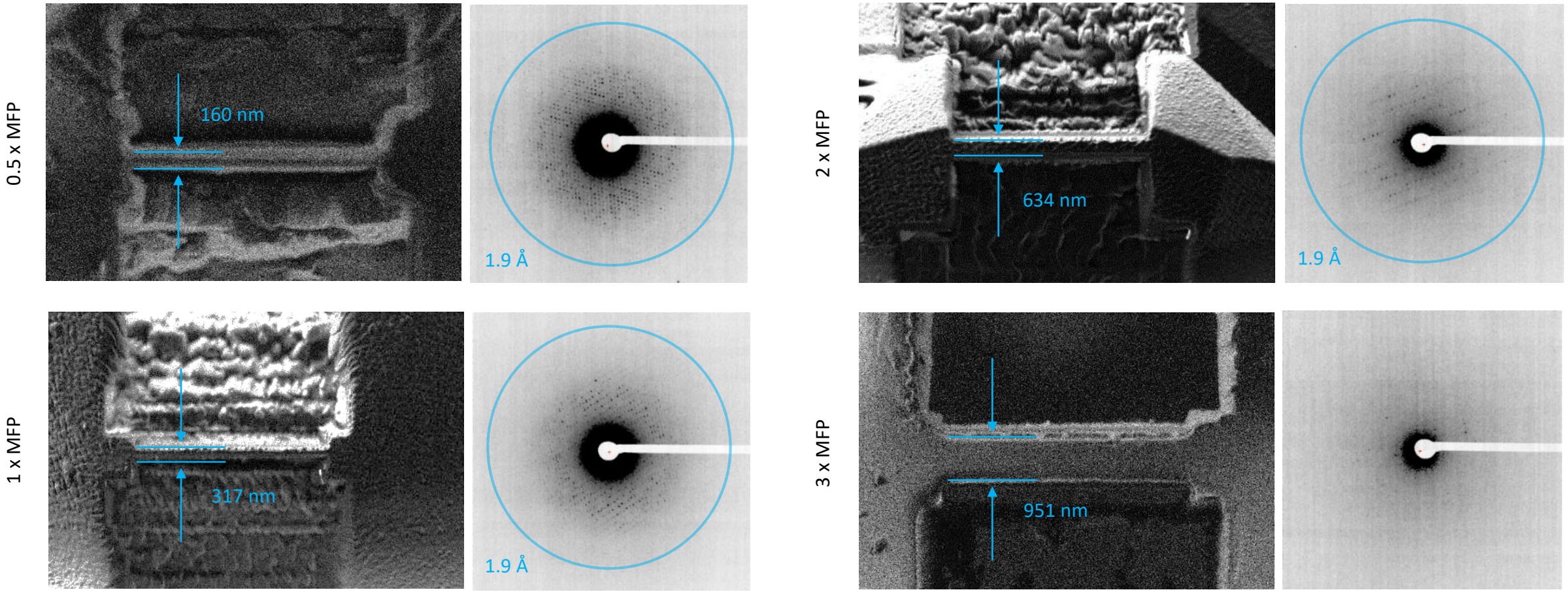

1× inelastic mean free path (MFP) at 300 kV is approximately 312 nm

High-quality data up to 2× the inelastic mean free path (MFP)

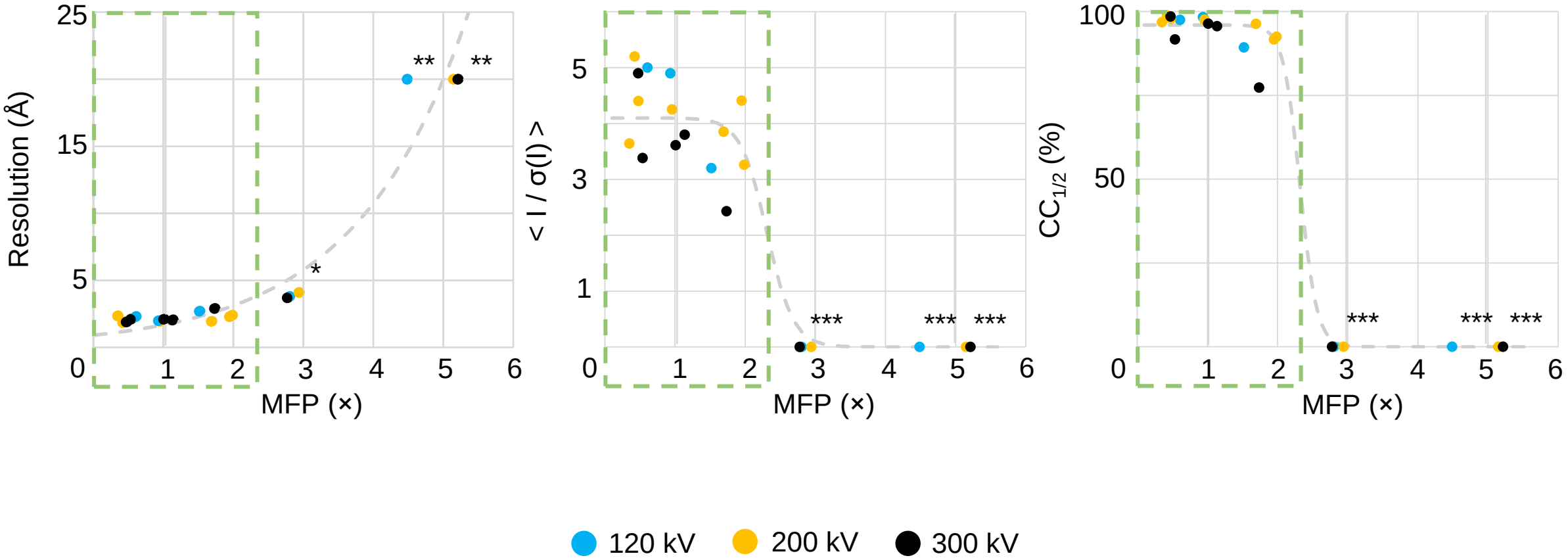

Electron crystallography of membrane protein crystals

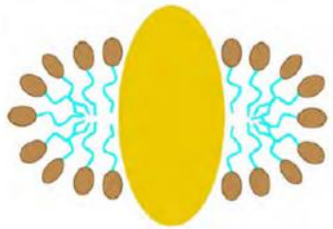

Detergent micelle

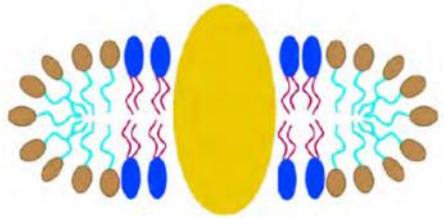

Detergent-lipid bicelle

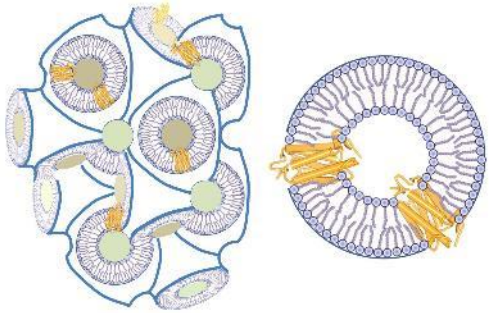

Lipidic cubic phase (LCP)

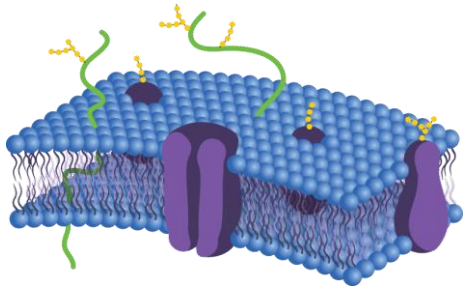

Lipid bilayer

Increasing difficulty

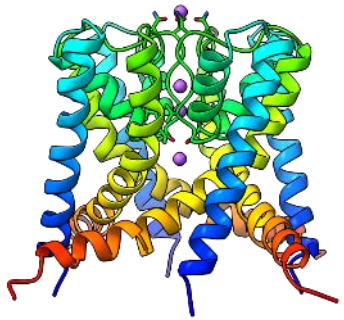

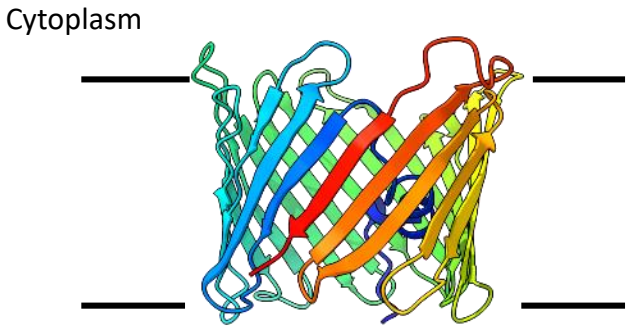

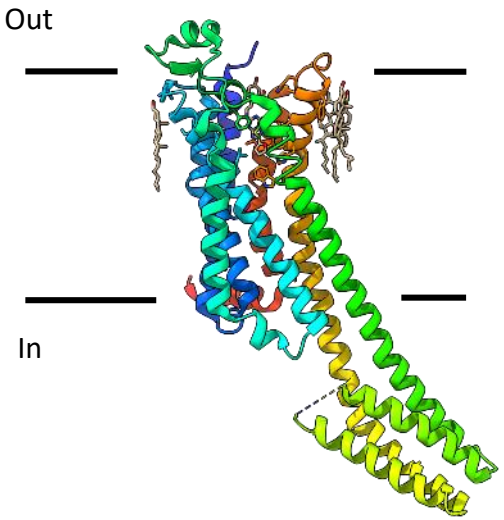

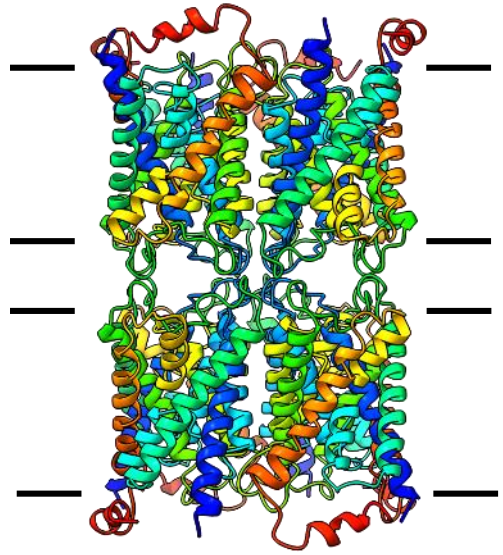

Locating protein crystals embedded in highly viscous detergent-lipid bicelles

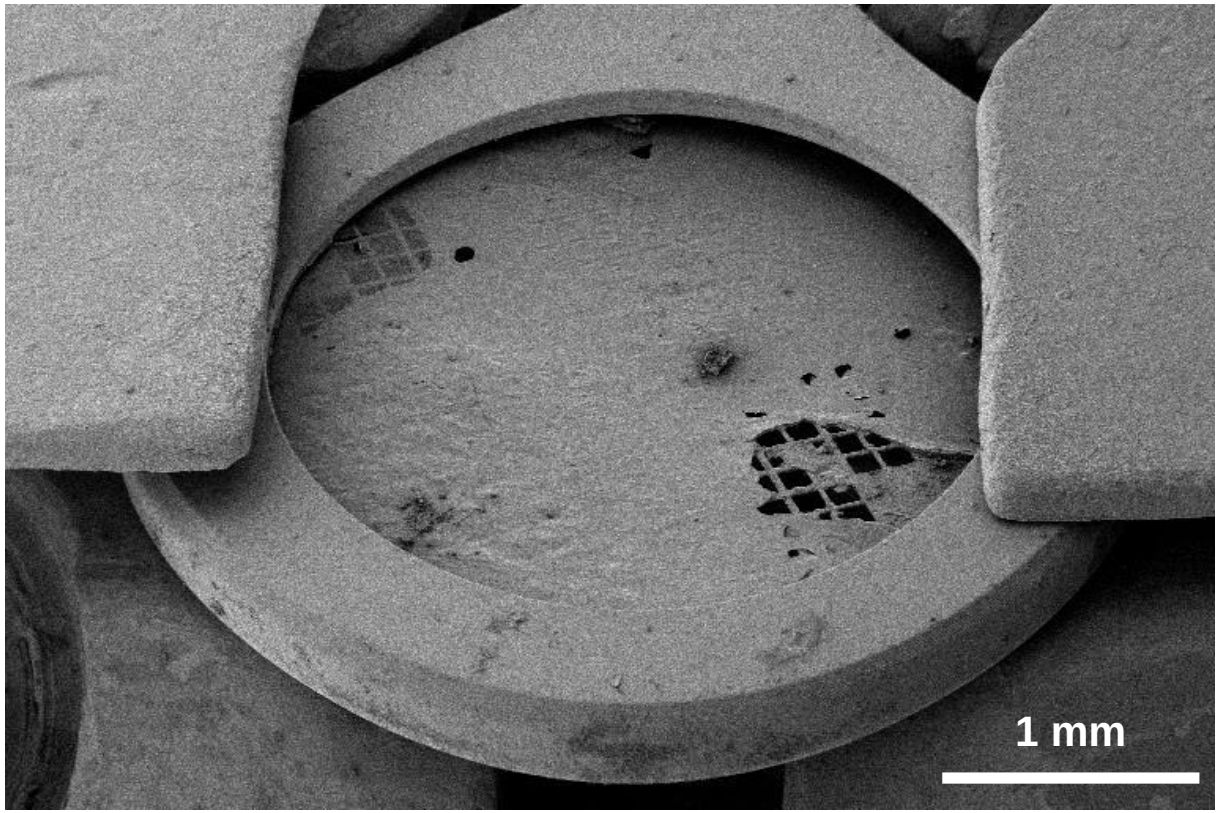

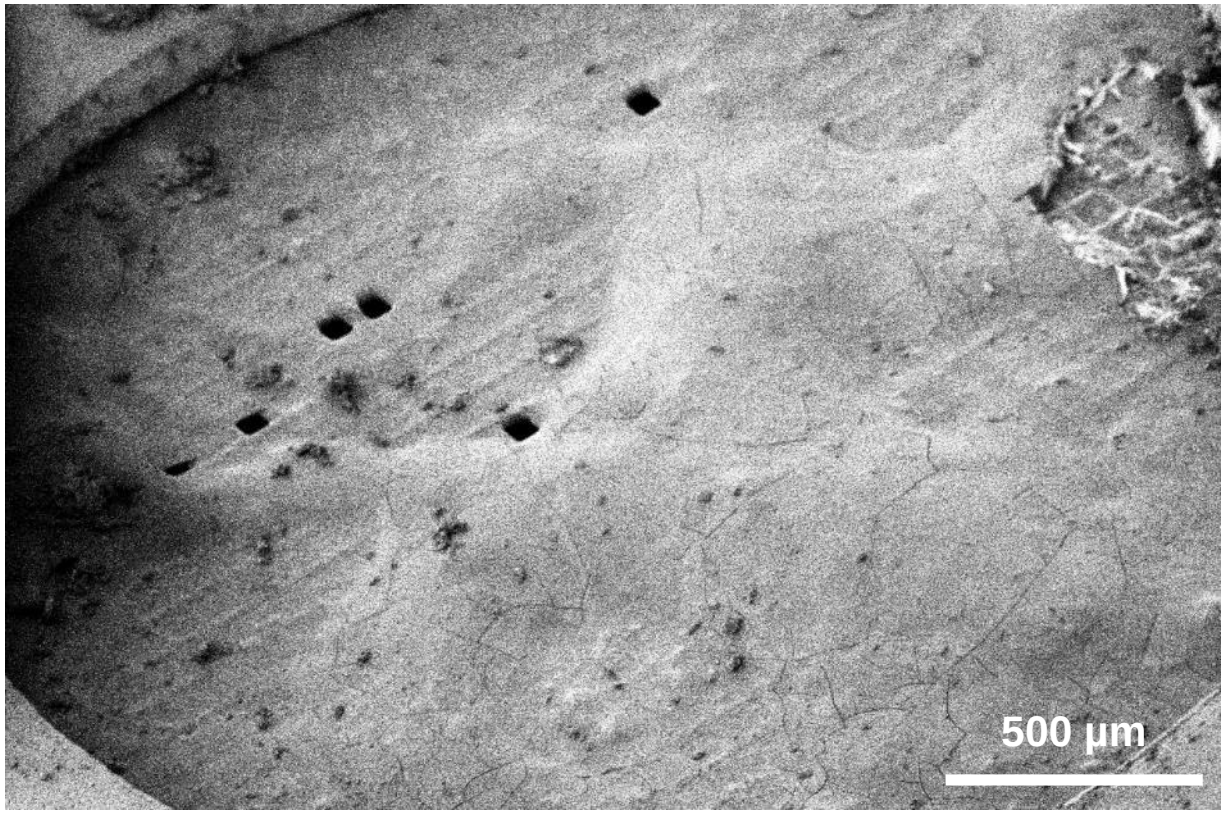

Martyonowycz *et al.*, *PNAS* 117, 32380-32385 (2020)

Uncovering the embedded crystals using a dual-beam FIB/SEM

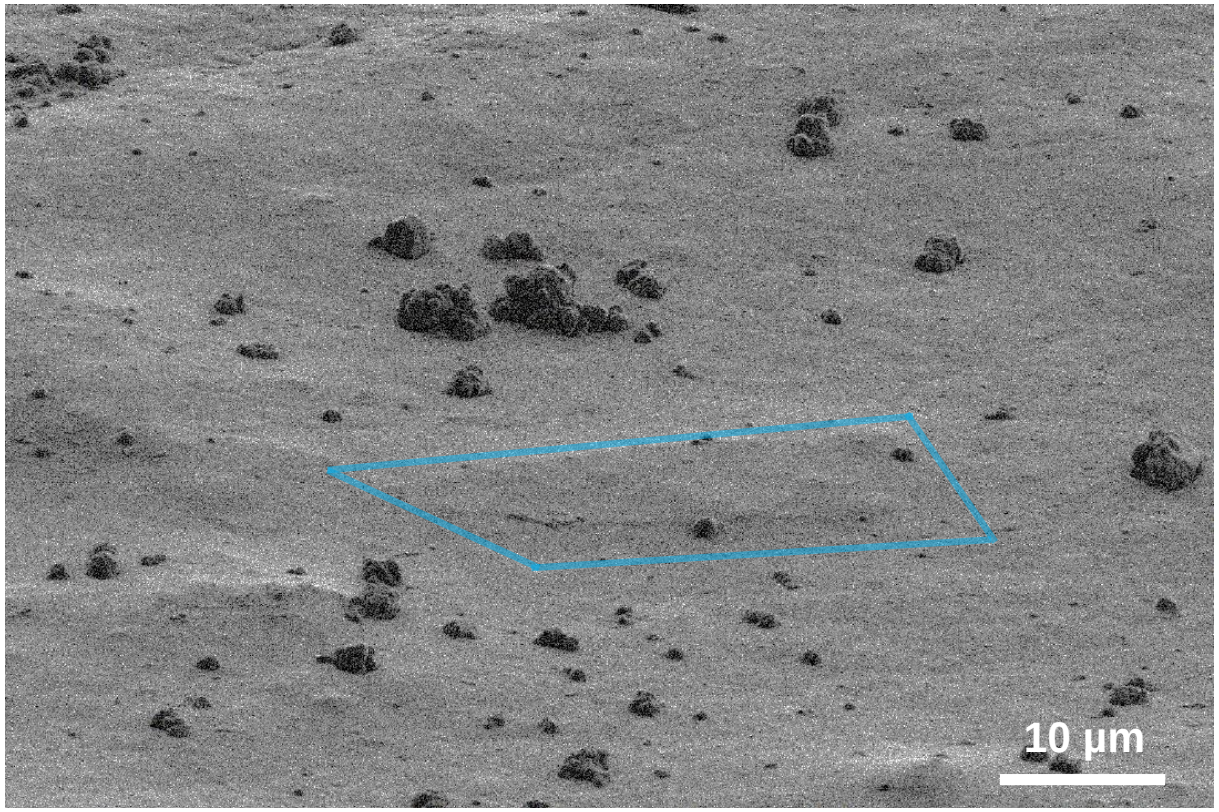

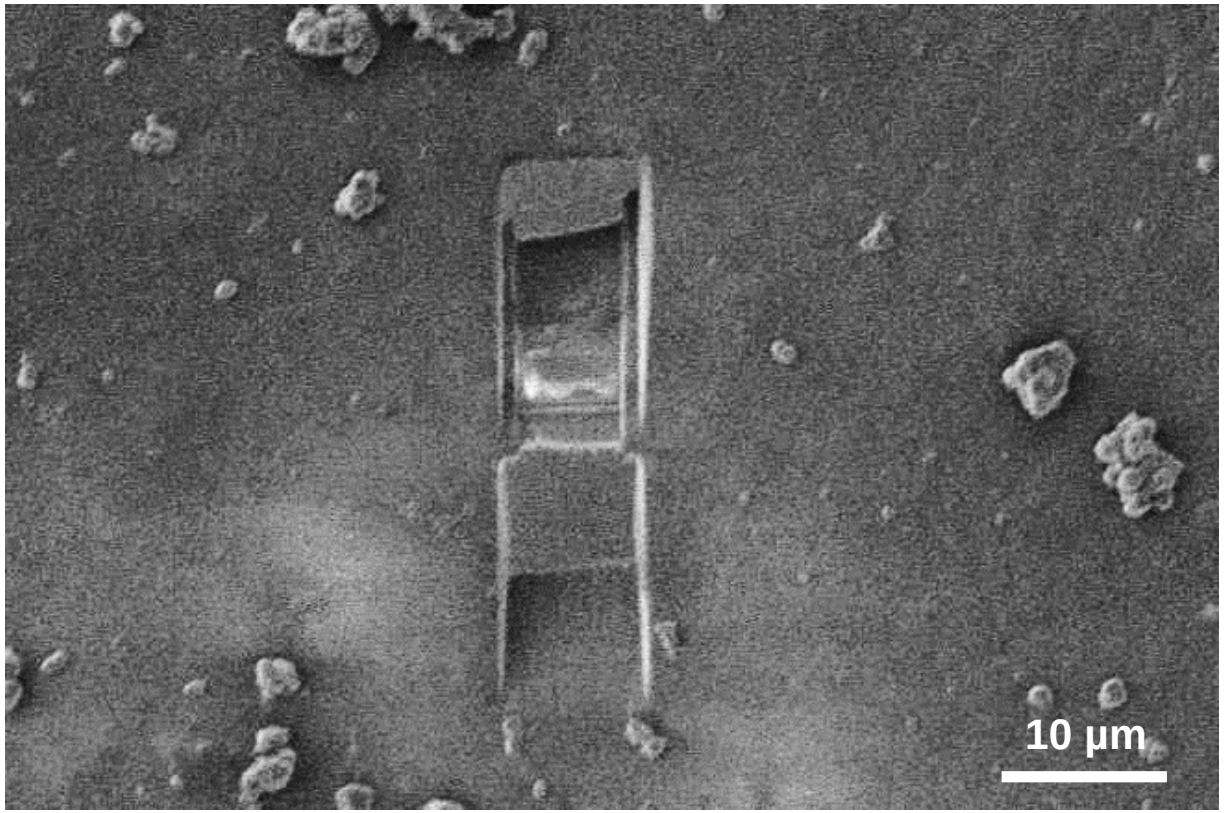

Martyonowycz *et al.*, *PNAS* 117, 32380-32385 (2020)

Structure of the lipid-embedded mammalian mitochondrial voltage-dependent anion channel

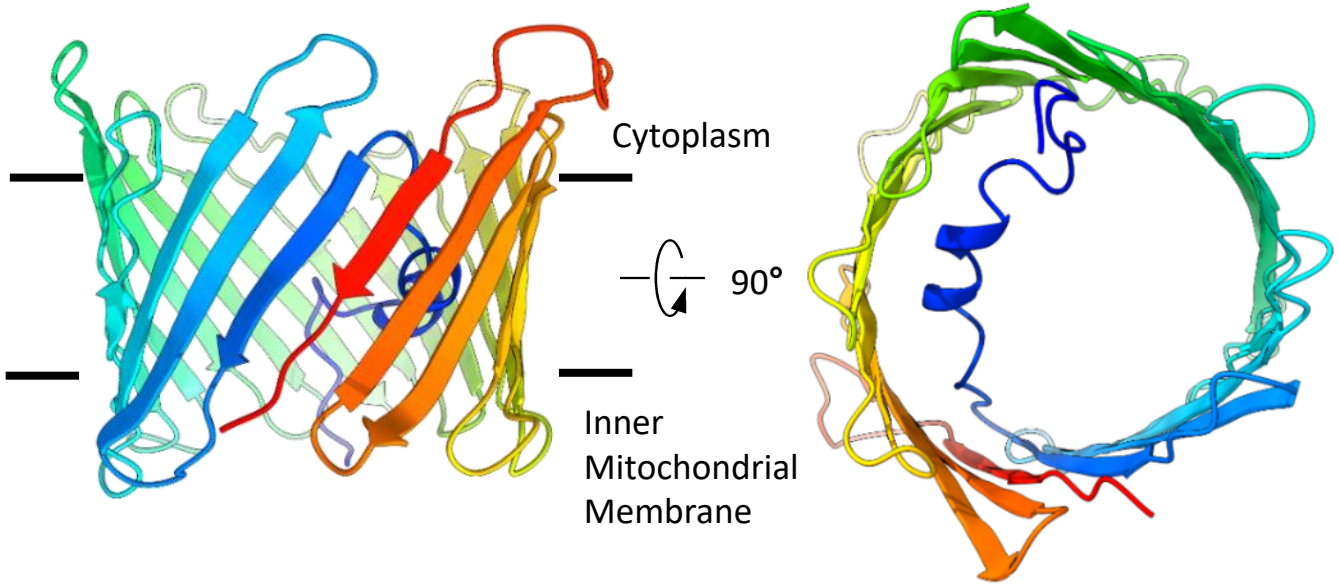

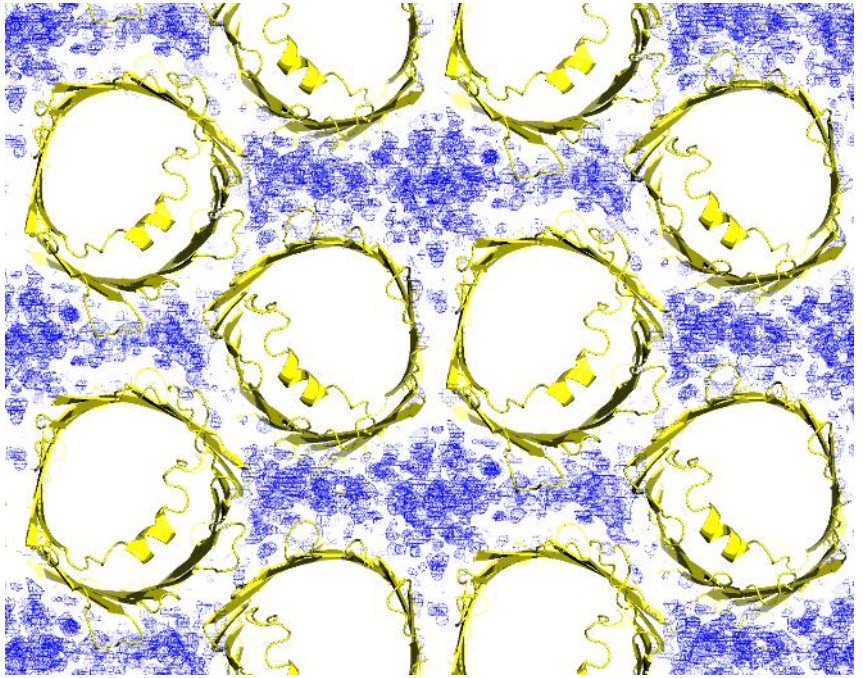

Martyonowycz *et al.*, *PNAS* 117, 32380-32385 (2020)

Phase conversion of lipid cubic phase (LCP) crystals to a less viscous sponge phase

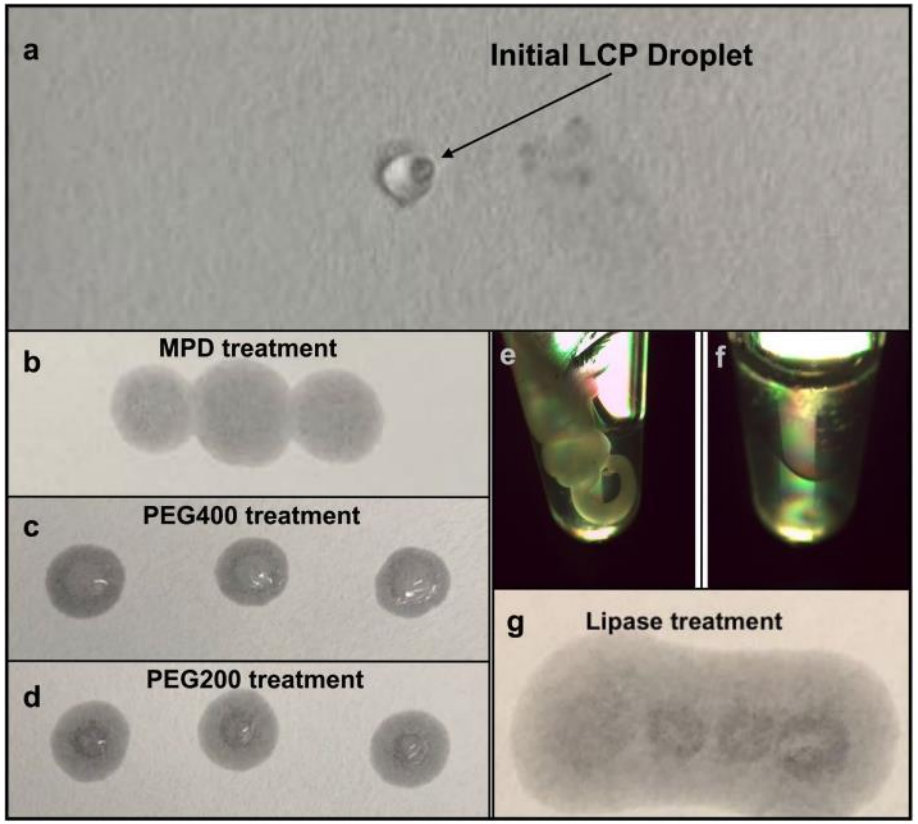

Zhu *et al.*, *Structure* 28, 1-11 (2020)

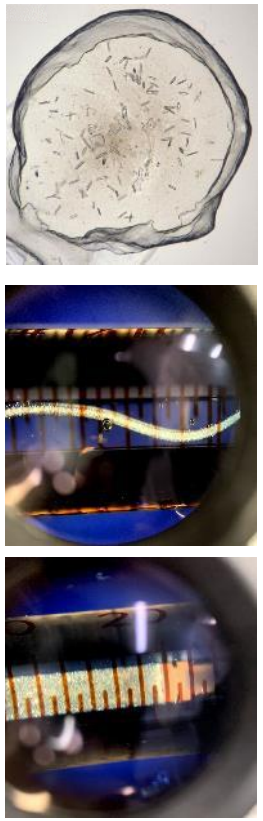

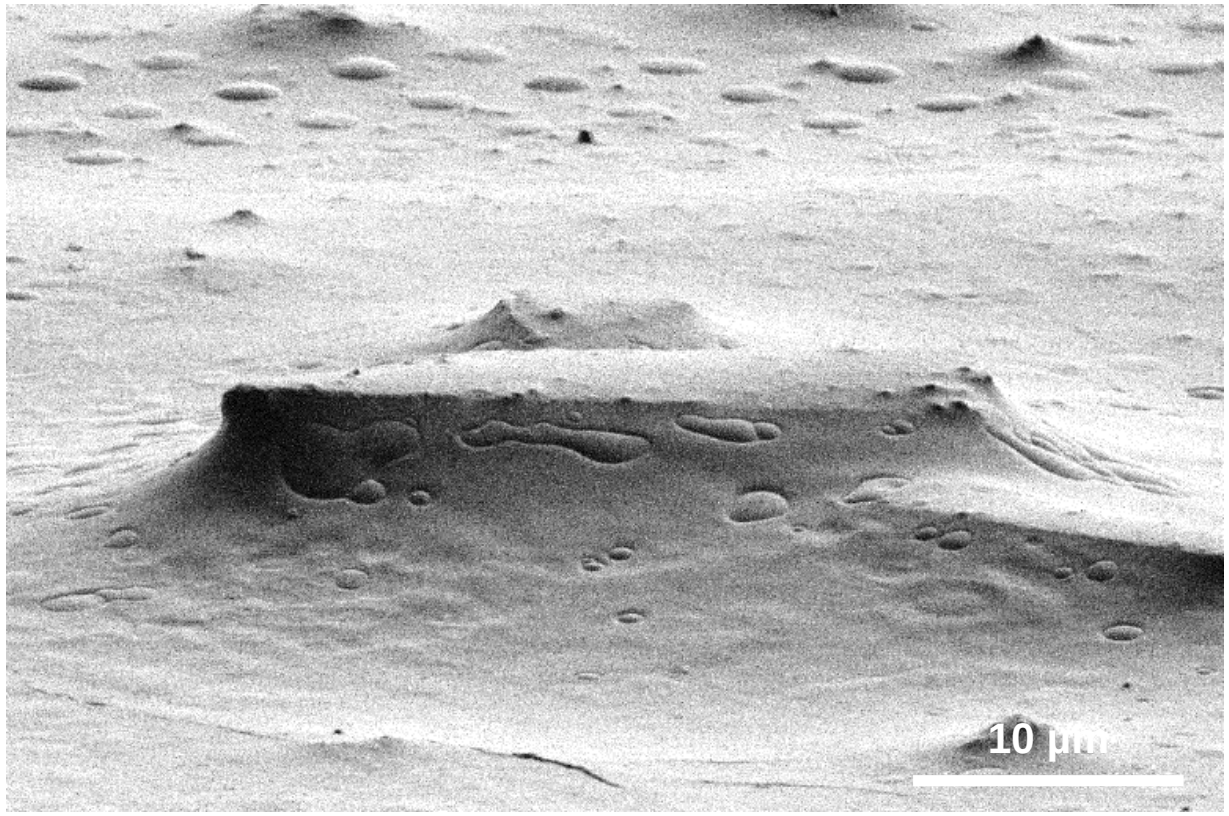

Martyonowycz *et al.*, *PNAS* 118, e2106041118 (2021)

Targeting GPCR crystals embedded in LCP using pFIB/SEM with integrated FLM module

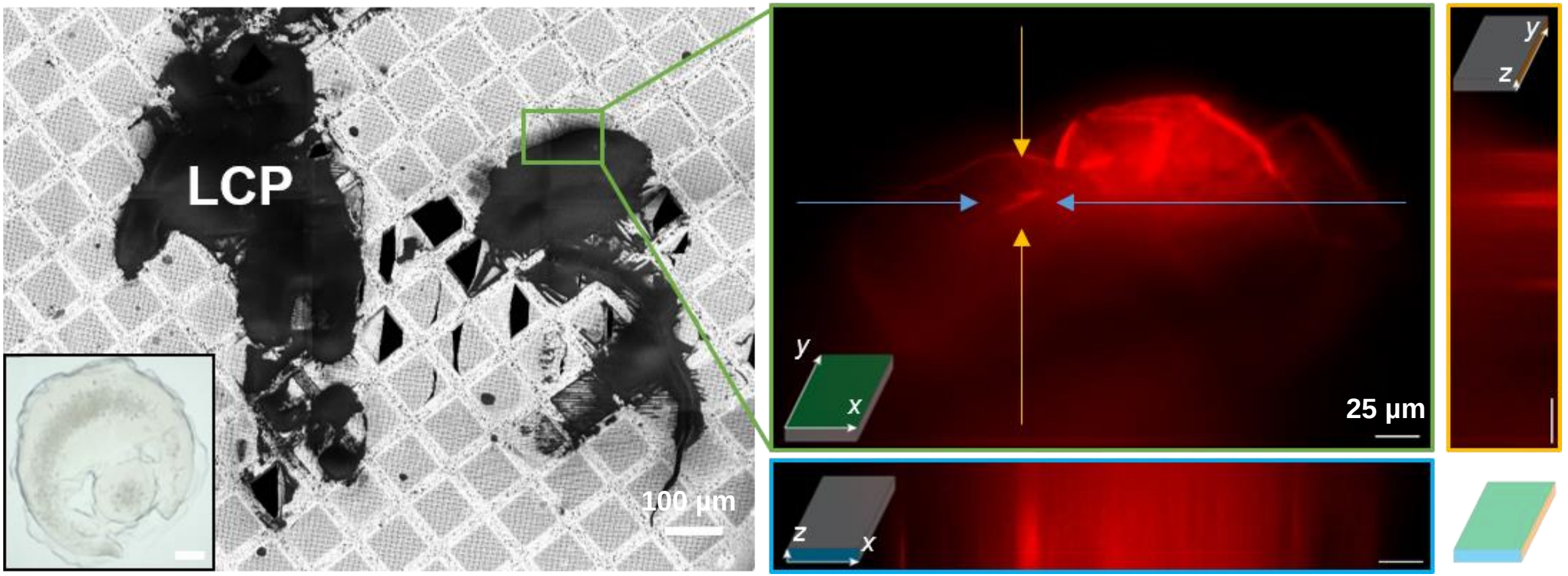

Localizing crystals embedded in LCP by correlating SEM images and FLM stacks

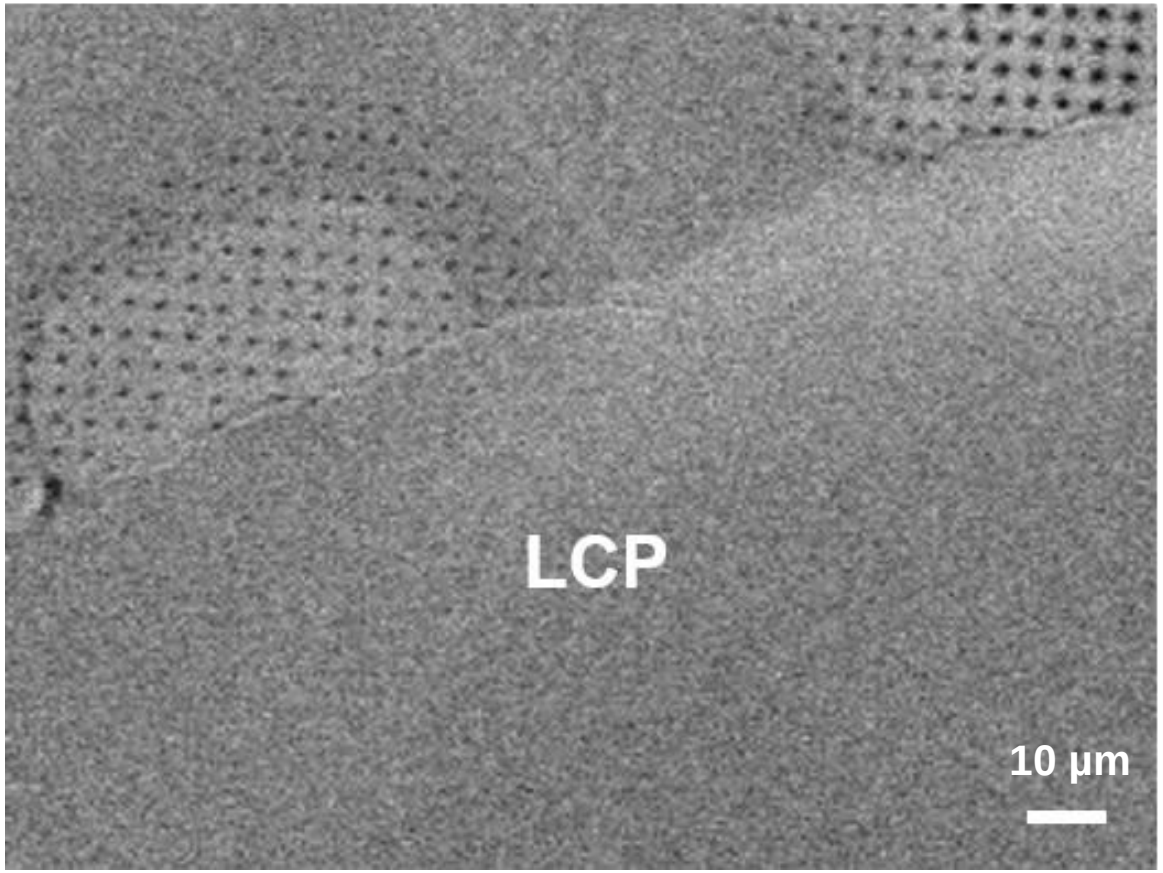

SEM

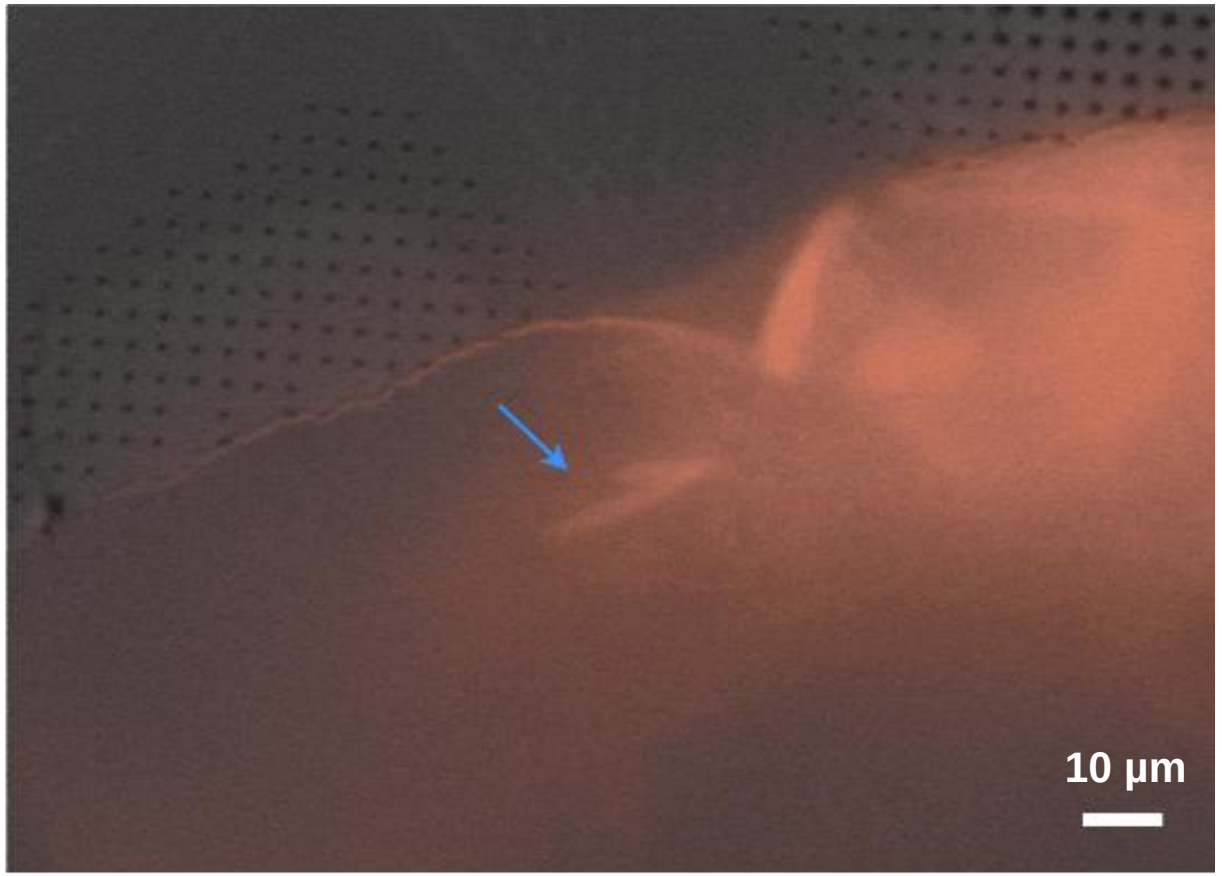

SEM+FLM

Using plasma FIB milling to target and access the crystals directly in LCP

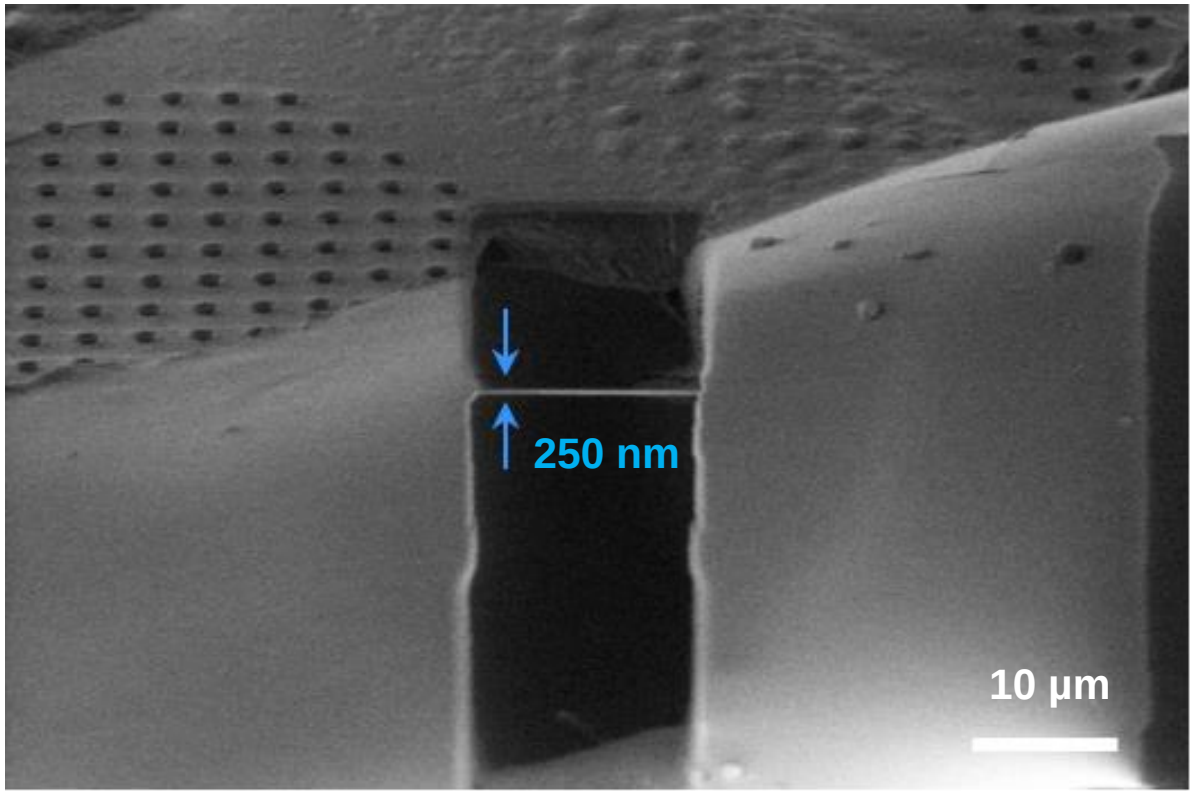

SEM

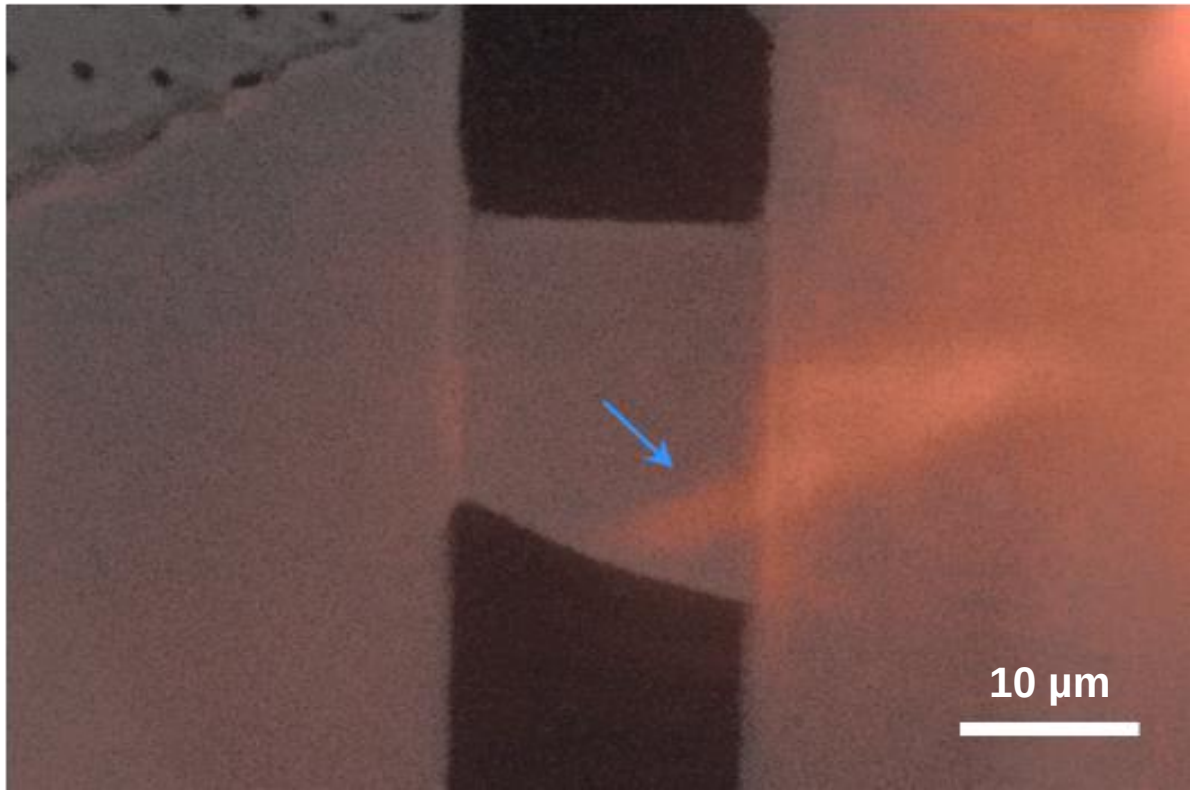

SEM+FLM

Structure of the human adenosine receptor $A_{2A}AR$ at 2.0 Å resolution

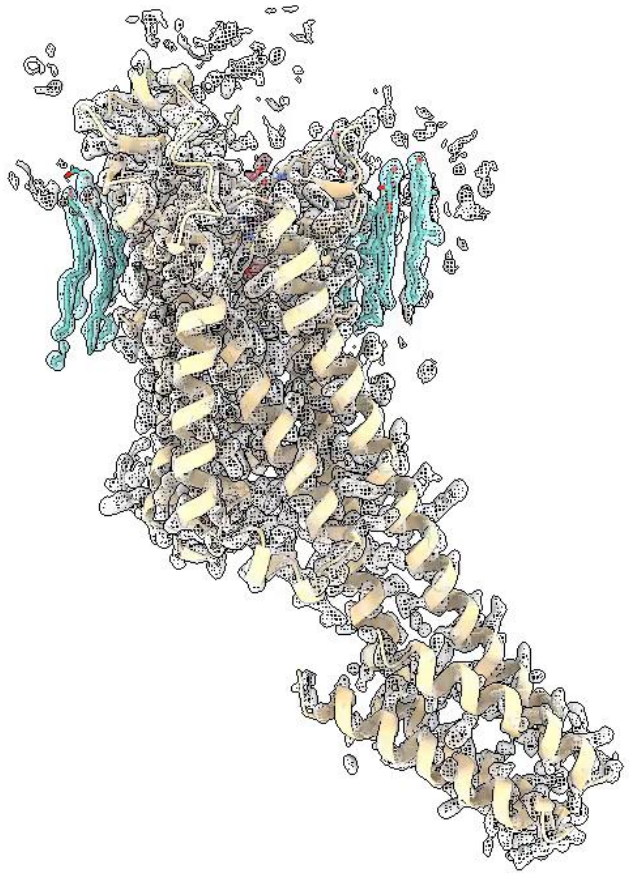

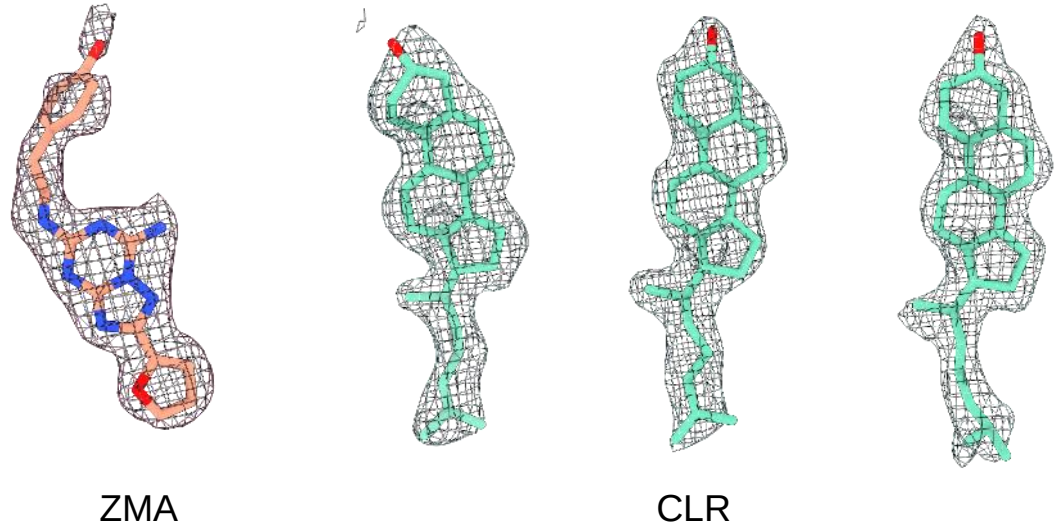

ZMA

CLR

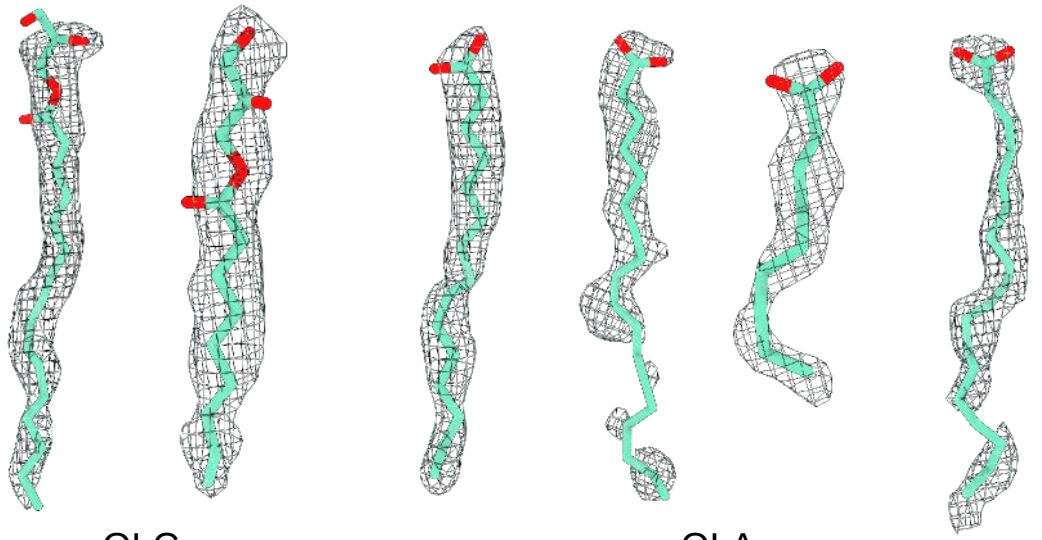

OLC

OLA

Optimized sample preparation workflow for fluorescently labeled microcrystals

Vitrification

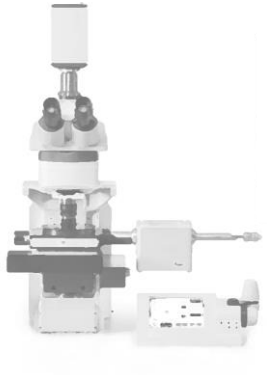

CLEM

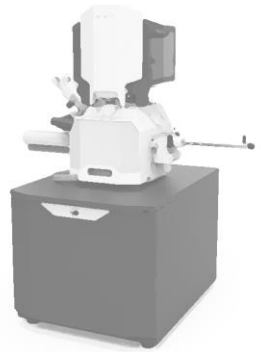

FIB/SEM

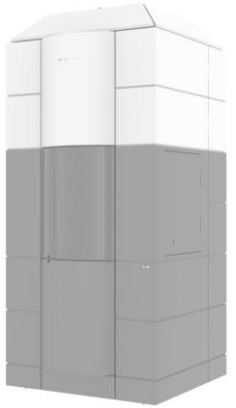

Cryo-EM

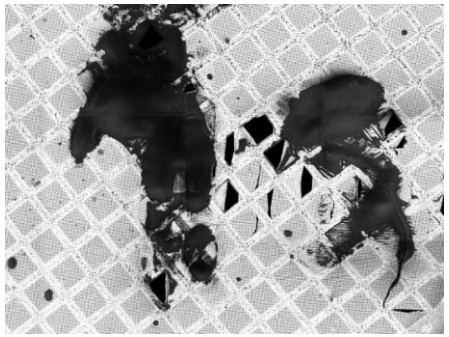

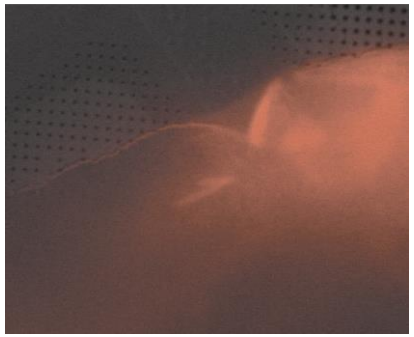

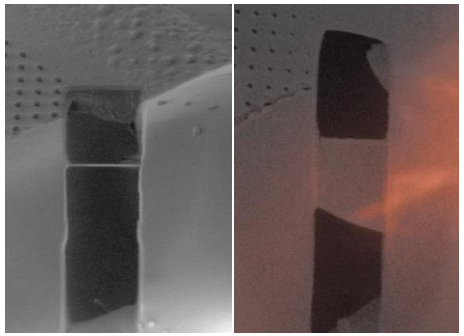

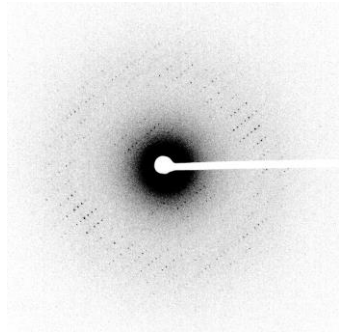

The continuous rotation method in MicroED is analogous to X-ray crystallography

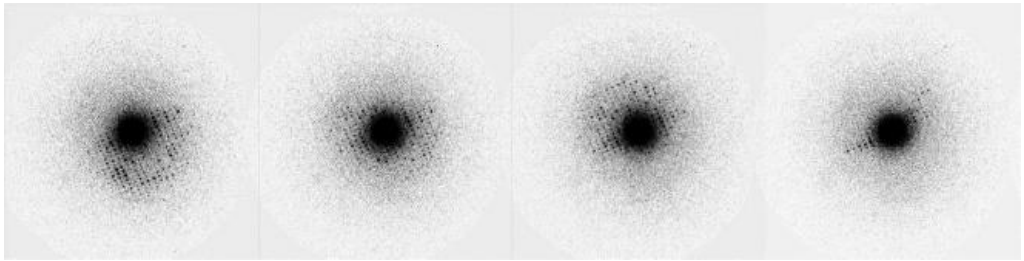

Continuous rotation electron diffraction data collection of protein nanocrystals using a hybrid pixel detector

Nederlof *et al.*, *Acta Cryst.* D69, 1223-1230 (2013)

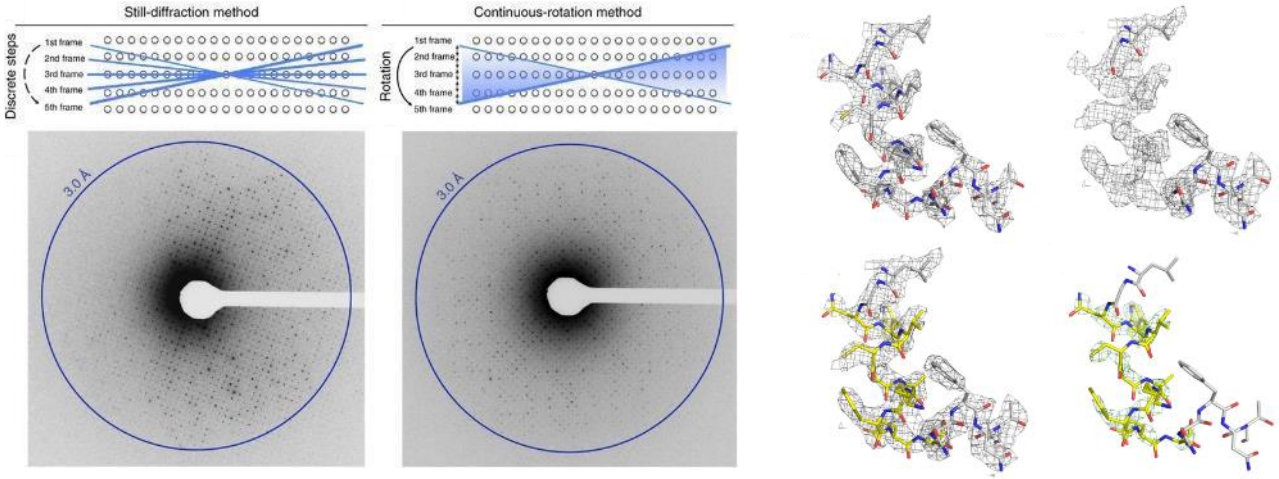

Continuous rotation MicroED data collection and structure determination from protein microcrystals

Nannenga *et al.*, *Nat. Methods* 11, 927-930 (2014)

Radiation damage for crystalline biological specimens in electron microscopy

Global and site-specific radiation damage

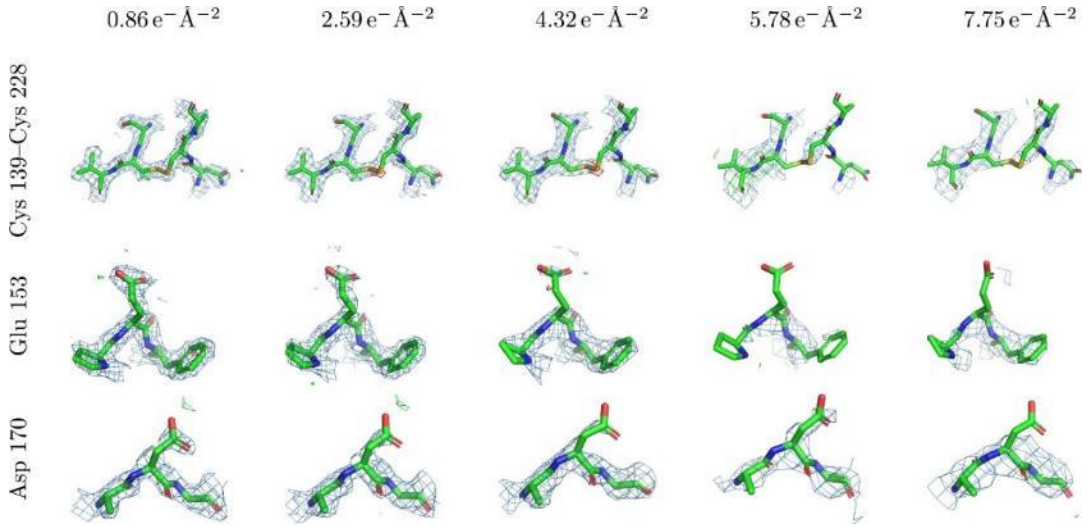

Half of the mean diffracted intensity is lost after an exposure of ~2.2 $e^-/Å^2$

Hattne *et al.*, *Structure* 26, 759-766 (2018)

Dose fractioning for optimal data quality

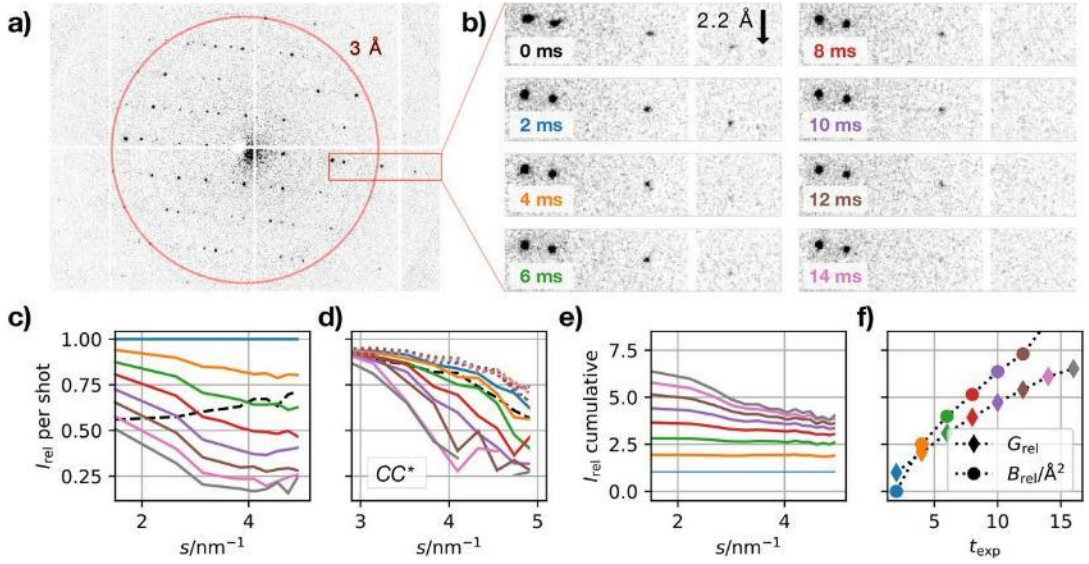

Optimal data quality at an exposure of ~2.6 $e^-/Å^2$ for lysozyme microcrystals, and ~4.7 $e^-/Å^2$ for granulovirus occlusion bodies

Buecker *et al.*, *Nat. Commun.* 11, 996 (2020)

Camera requirements for continuous MicroED data collection

Continuous rotation requires rapid readout

- ❑ Less gaps are introduced in the data
- ❑ Even if camera supports gapless data collection, data collection software may not

Diffraction can sacrifice spatial resolution

- ❑ Depending on unit cell size and resolution

Diffraction requires high dynamic range

- ❑ Spots are strong, background is faint

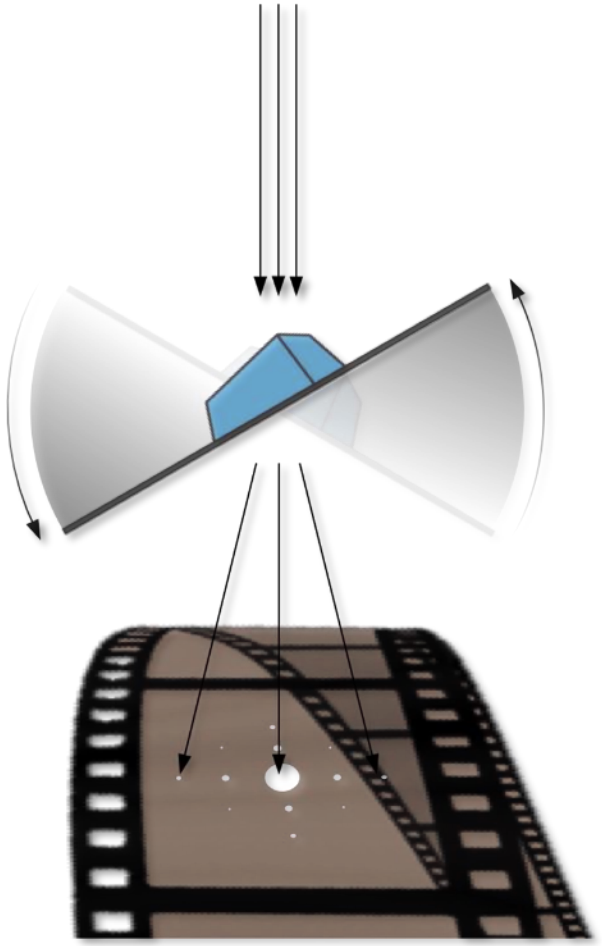

Exposure, frame rate, and linear range for electron-counting cameras

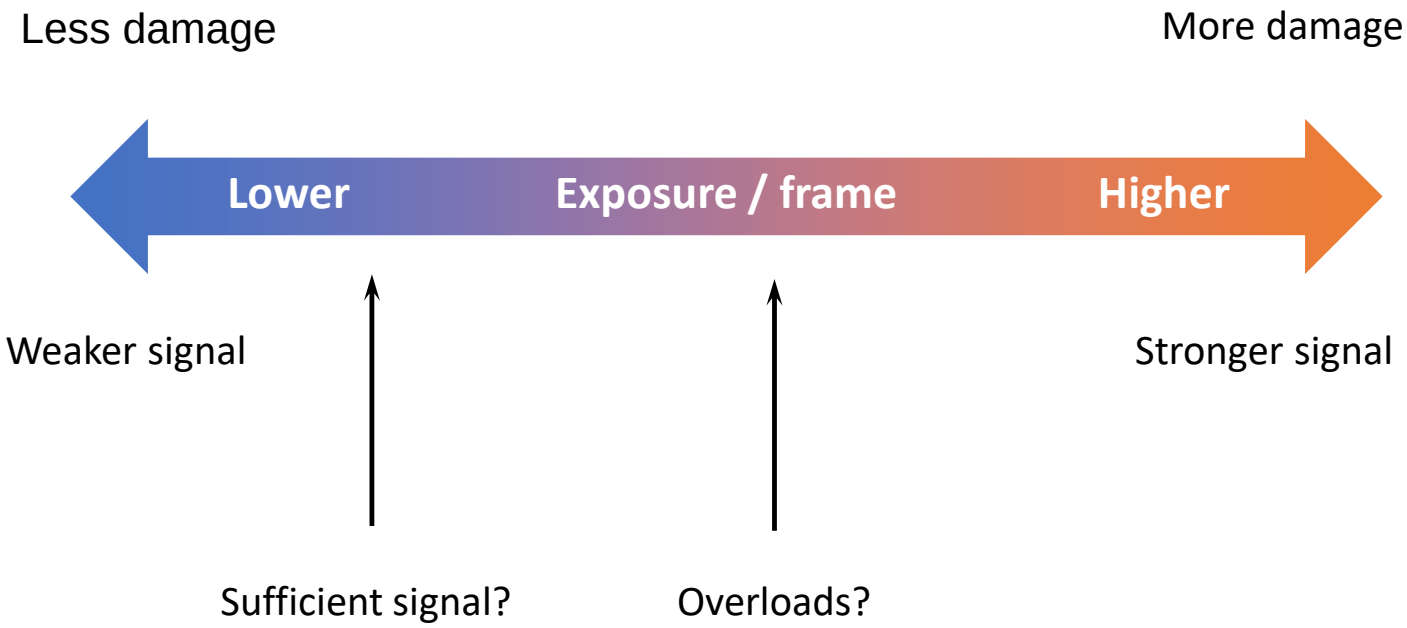

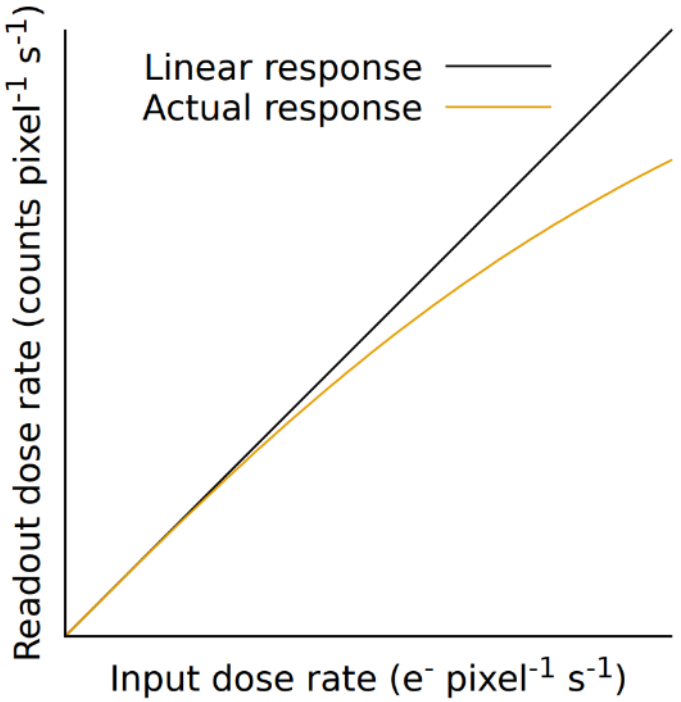

Facilitating low exposure electron-counting MicroED data collection

Lower the exposure rate to sample

- ❑ Smaller C2 aperture
- ❑ Larger spot size
- ❑ Larger beam size

Reduce counts on camera

- ❑ Use selected area (SA) aperture

Improve low count statistics

- ❑ Extend the exposure time
- ❑ Optimize SNR using FIB/SEM

Beyond molecular replacement

Whereas structures of short peptide fragments can be solved by direct methods from MicroED data,
to date - all macromolecular structures have been phased by molecular replacement

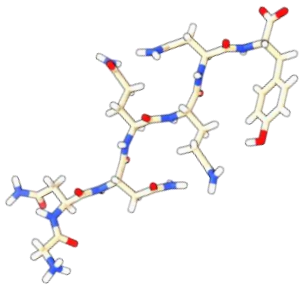

GNNQQNY (5K2N)

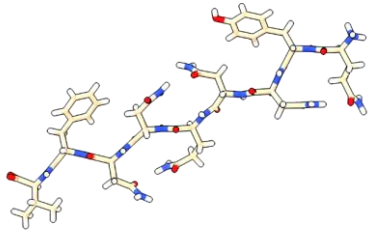

QYNNQNNFV (6AXZ)

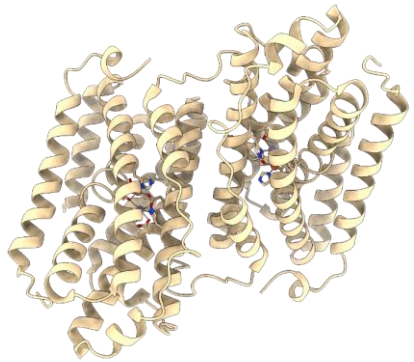

R2lox (6QRZ)

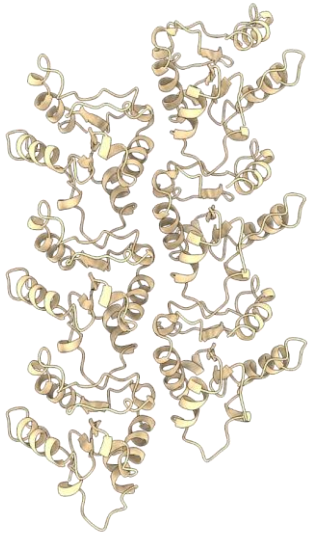

MyD88^{TIR} (7BEQ)

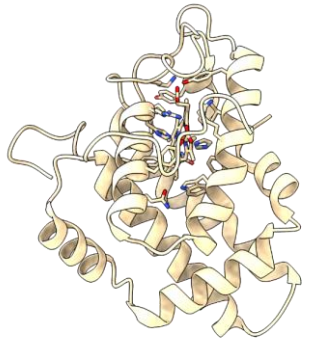

Protoglobin (7UTE)

Ab initio protein structure determination using electron-counted MicroED data

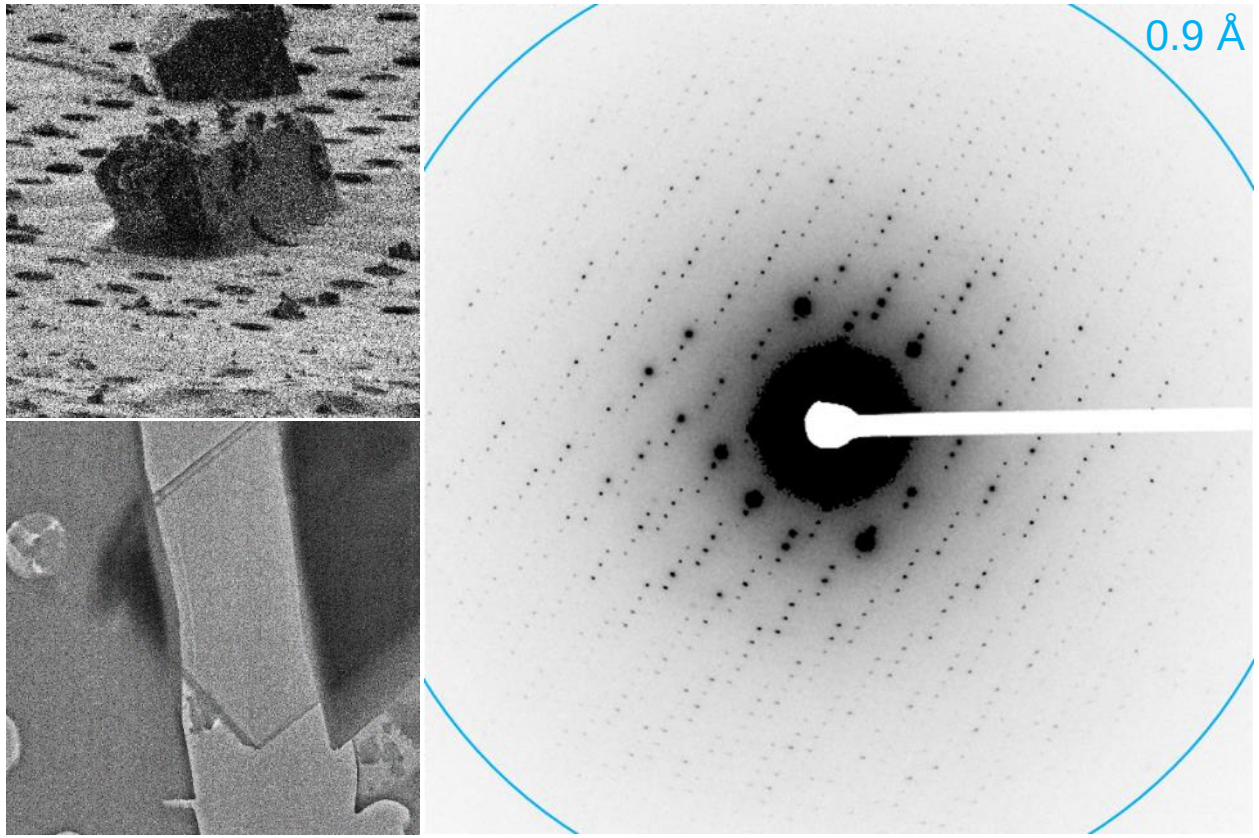

Triclinic lysozyme

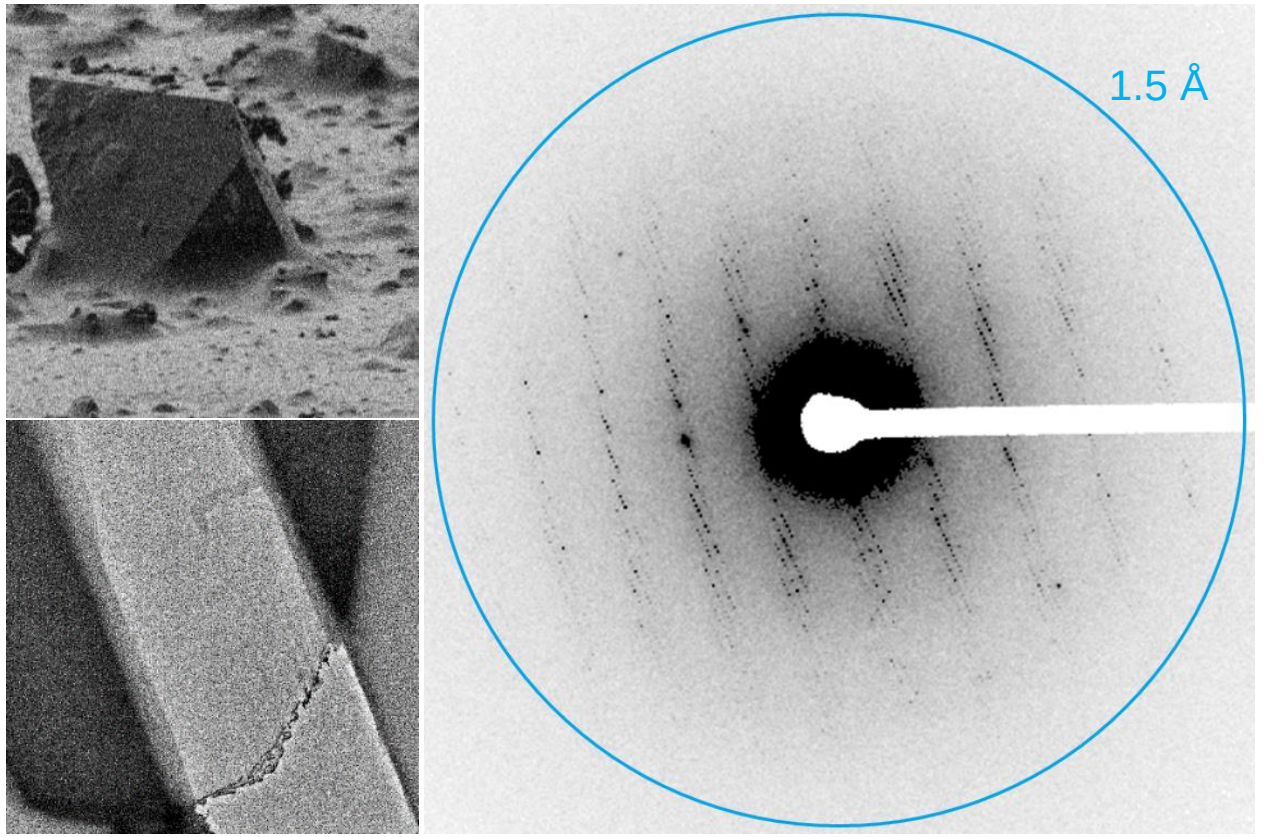

Proteinase K

Microscope setup for low exposure electron-counting MicroED data collection

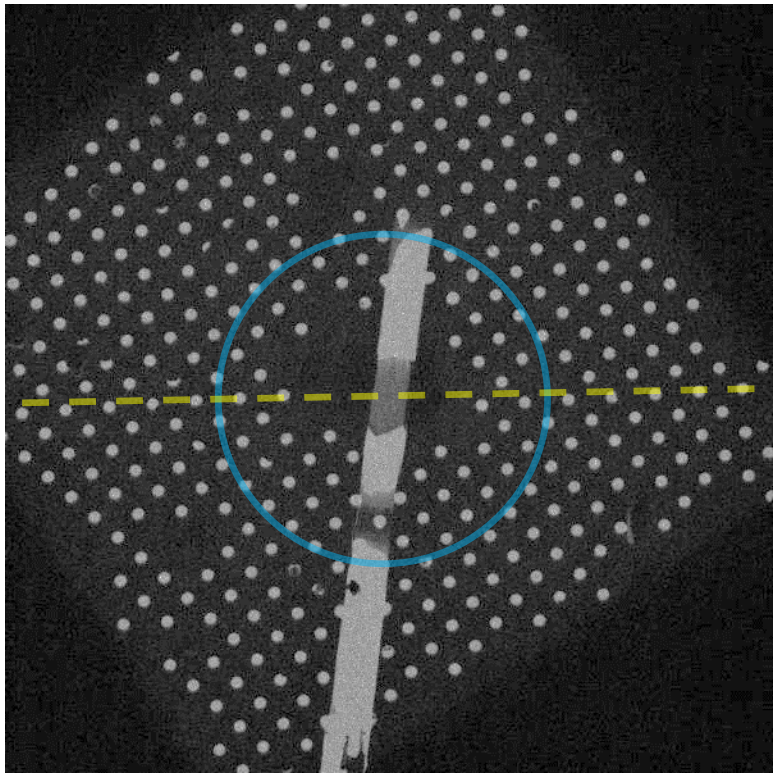

Spot size 11, 50 µm C2 aperture
25 µm diameter parallel beam

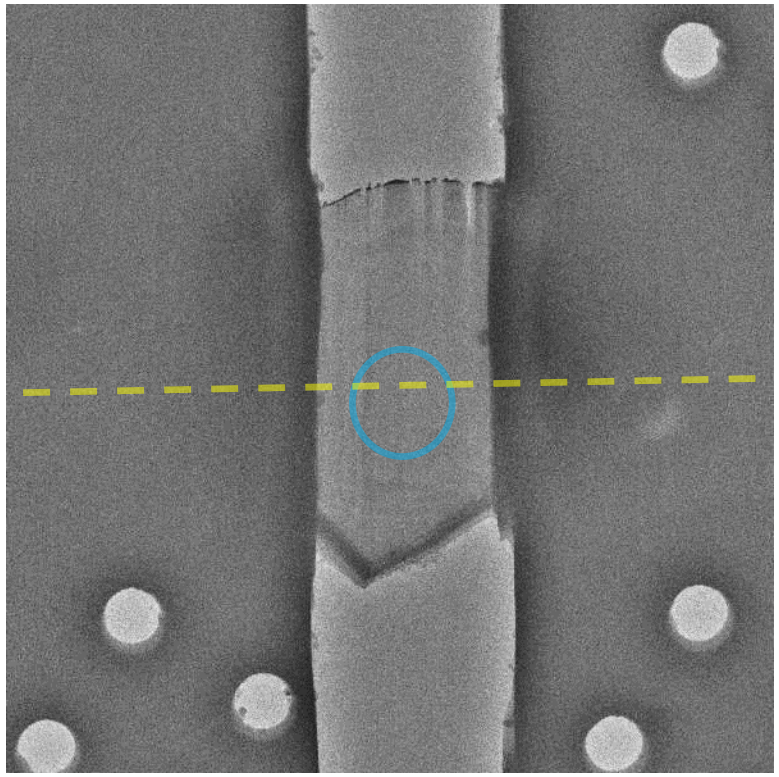

100 µm SA aperture
2 µm diameter at specimen

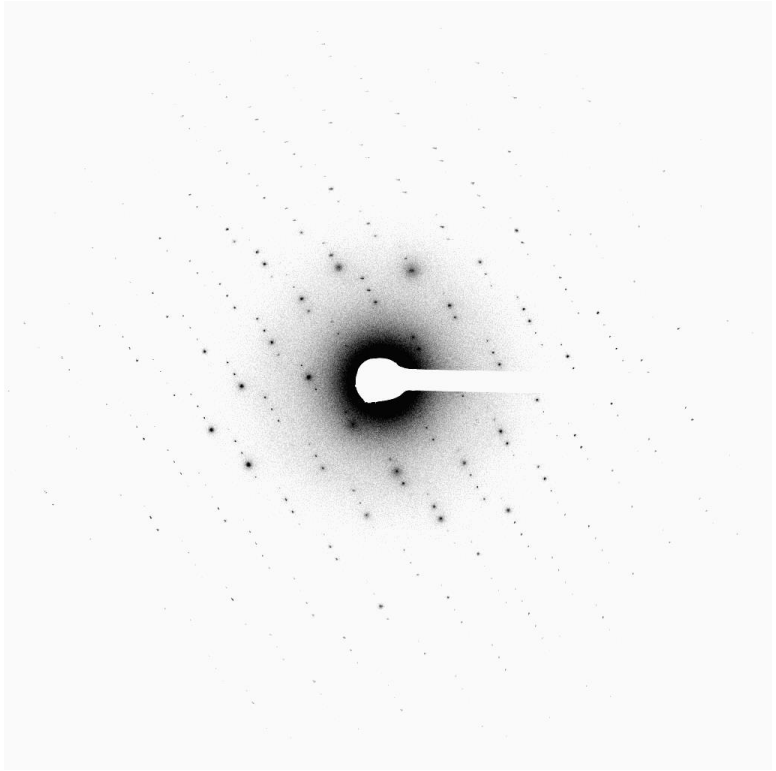

Falcon 4 (2× binning) in counting mode
84° rotation at 0.2 °/s
0.0015 $e^-/Å^2/s$ (total 0.64 $e^-/Å^2$)
420s exposure, 2fps readout

Data integration and merging of 16 crystal lamellae up to 0.87 Å resolution

No. of crystals	16
Space group	*P*1
Unit cell dimensions	
a, *b*, *c* (Å)	26.42, 30.72, 33.01
α, *β*, *γ* (°)	88.319, 109.095, 112.075
Resolution (Å)	16.05-0.87 (0.90-0.87)
Observed reflections	569407 (5797)
Unique reflections	64986 (2783)
Multiplicity	8.8 (2.1)
Completeness (%)	87.55 (37.64)
R_{merge}	0.236 (1.035)
R_{meas}	0.248 (1.409)
R_{pim}	0.073 (0.945)
<I/σI>	6.23 (0.66)
$CC_{1/2}$	0.990 (0.147)

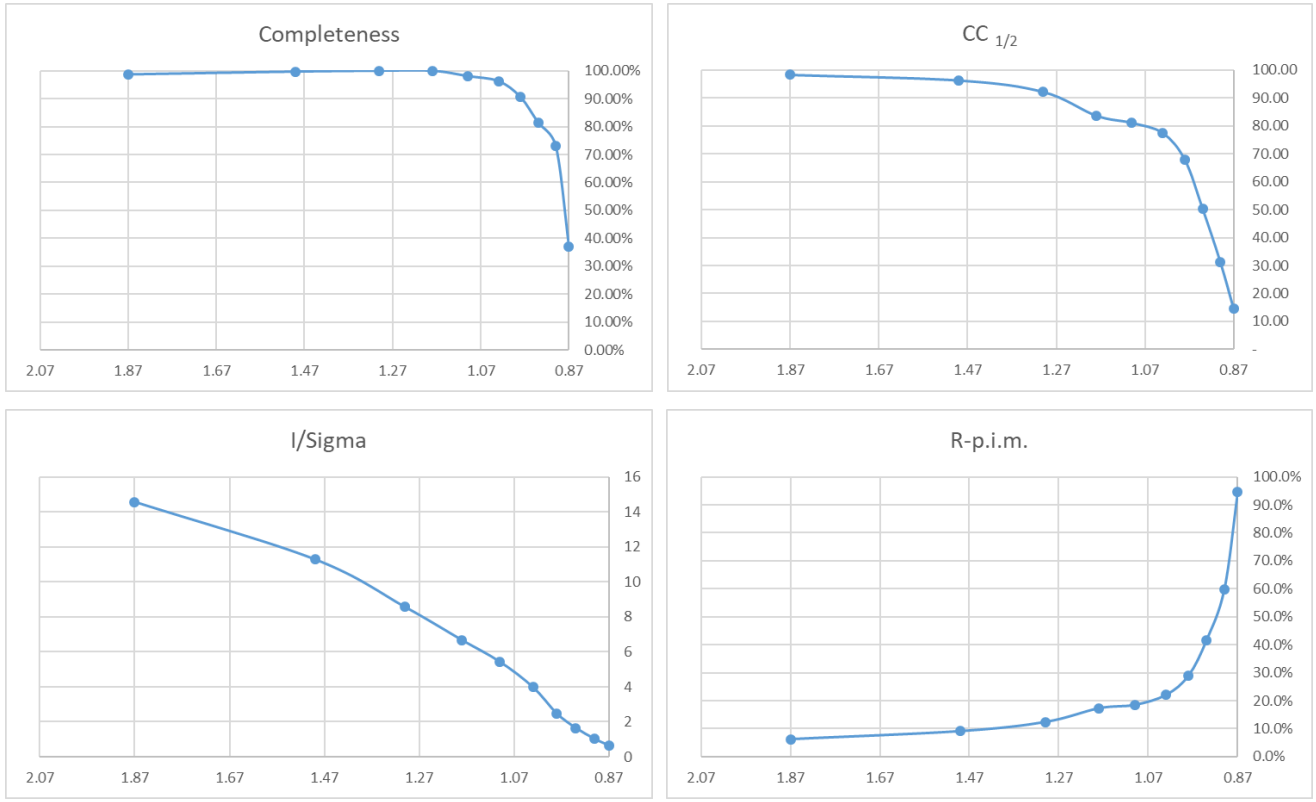

Ab initio phasing of triclinic lysozyme by placing an idealized starting fragment

Idealized starting fragment

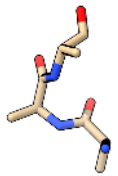

A single 3-residue helix (15 atoms)

Placing the fragment by MR

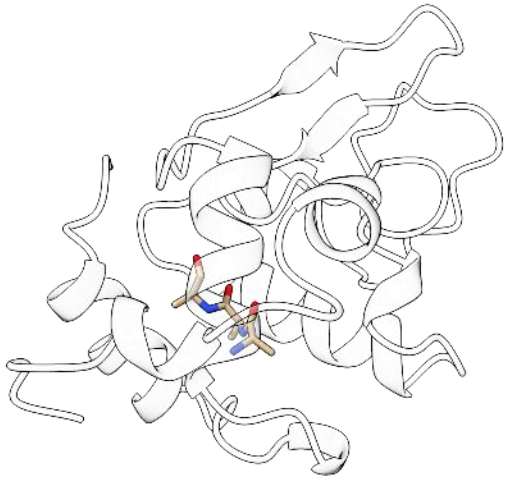

Solution from MR in *PHASER*

Initial map calculated from starting phases

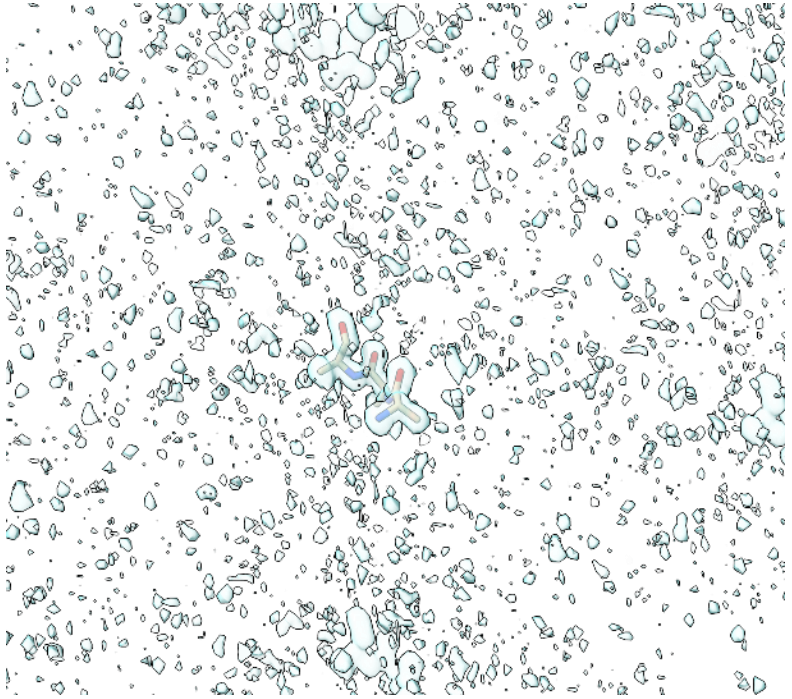

2mFo-DFc map

Phase improvement using dynamic density modification

Initial map after placing the idealized fragment

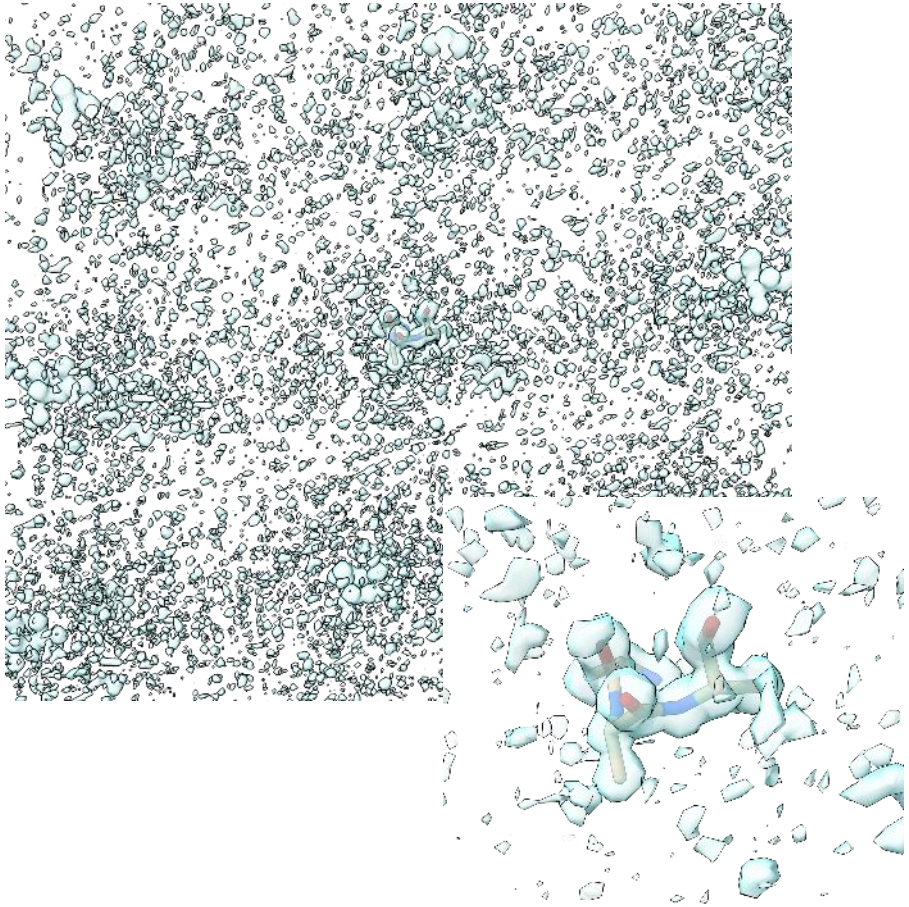

Density modified normalized structure factor map

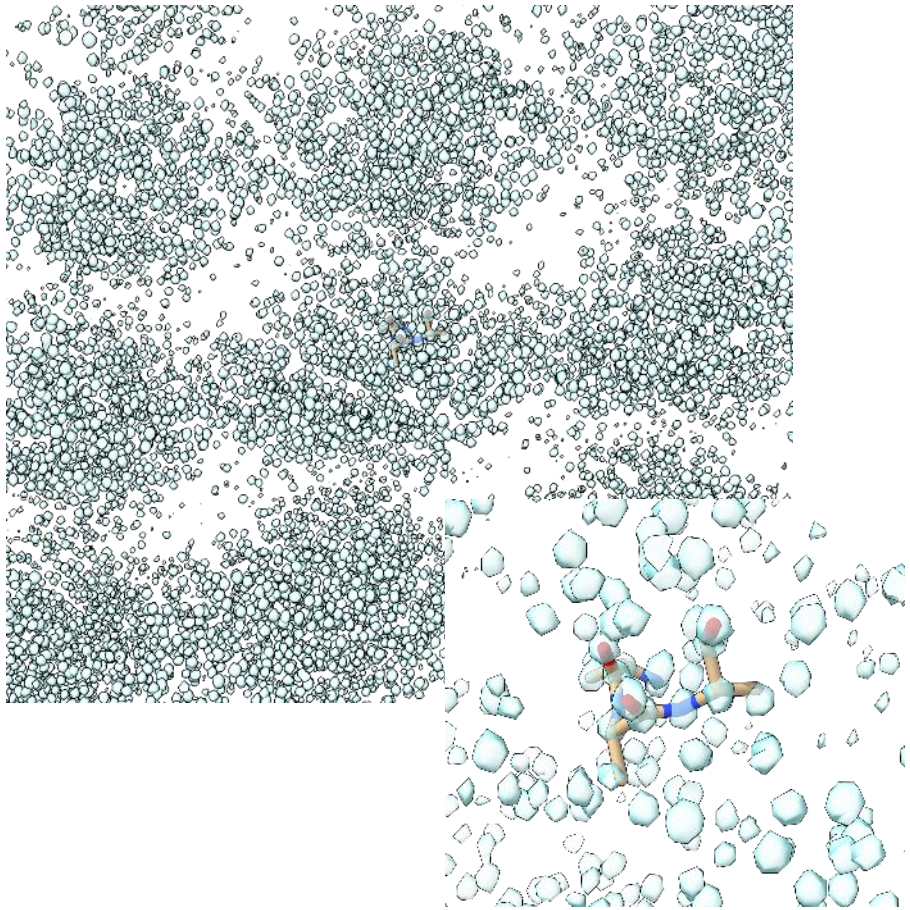

Automated model building and structure refinement

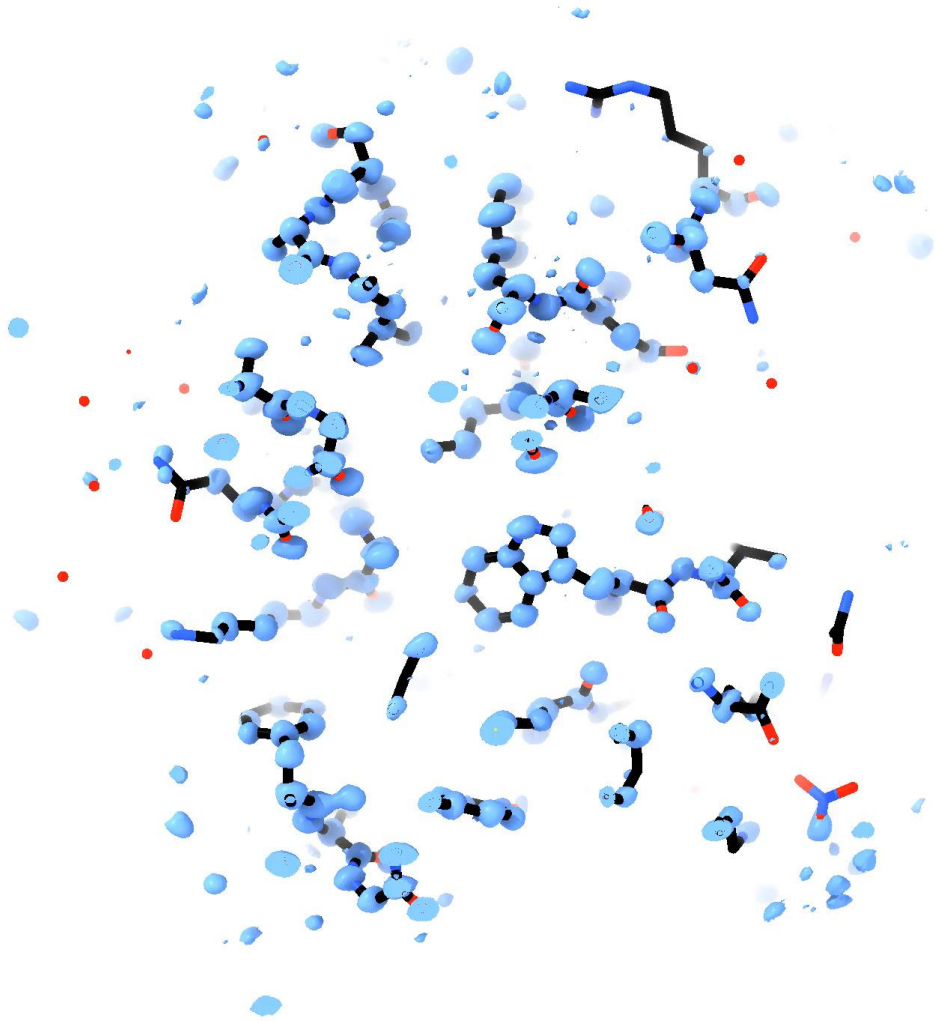

Automated model building and refinement using *BUCCANEER and REFMAC5*
0.87 Å resolution, R_{work}/R_{free} 0.179/0.231, 0.64 $e^{-}/Å^2$ total exposure

High-quality structural model of triclinic lysozyme at atomic resolution

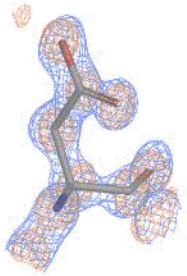

Aspartate (D)

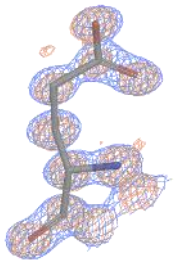

Glutamate (E)

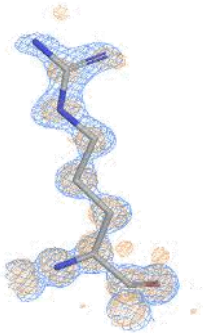

Arginine (R)

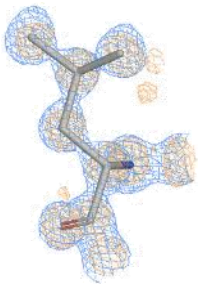

Leucine (L)

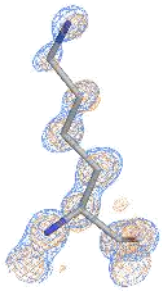

Lysine (K)

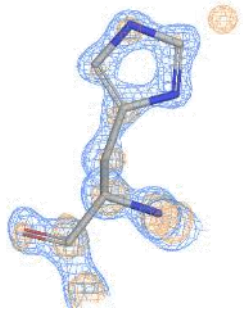

Histidine (H)

Phenylalanine (F)

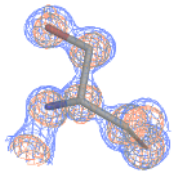

Serine (S)

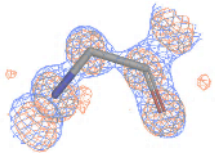

Glycine (G)

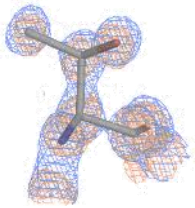

Threonine (T)

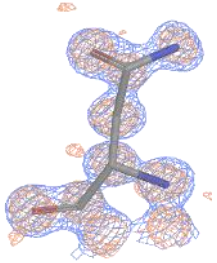

Asparagine (N)

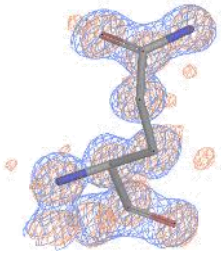

Glutamine (Q)

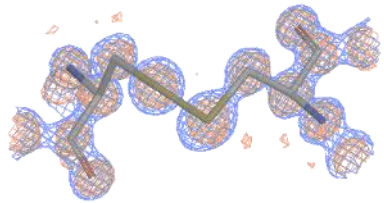

Cysteine – Cysteine (C)

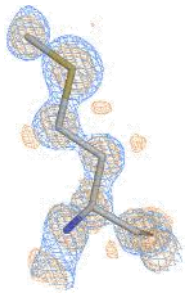

Methionine (M)

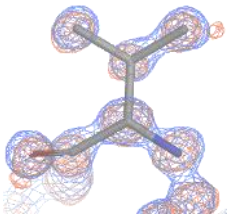

Valine (V)

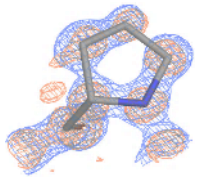

Proline (P)

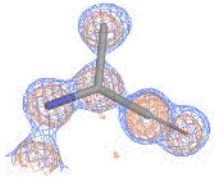

Alanine (A)

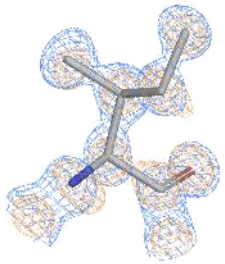

Isoleucine (I)

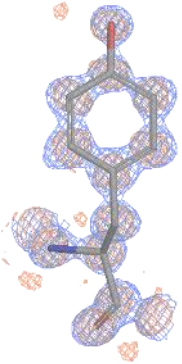

Tyrosine (Y)

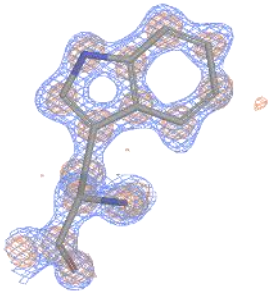

Tryptophan (W)

Density modified E map at 1.5σ, 2mFo-DFc map at 1.5σ

Hydrogen atom positions and hydrogen bonding interactions

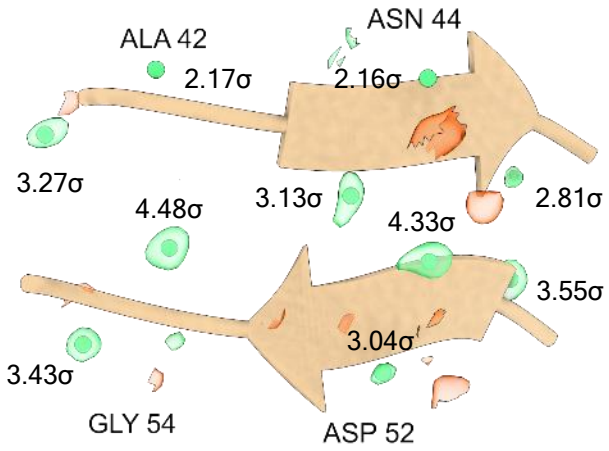

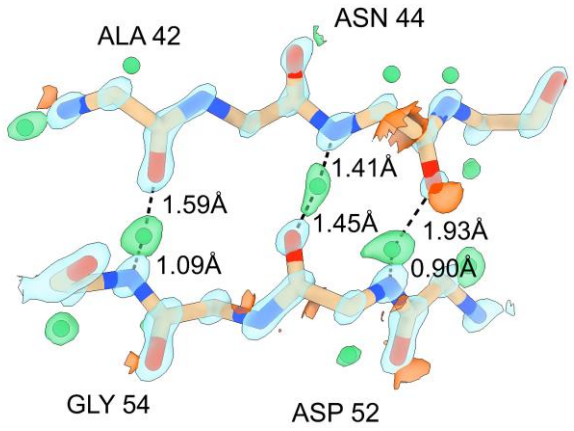

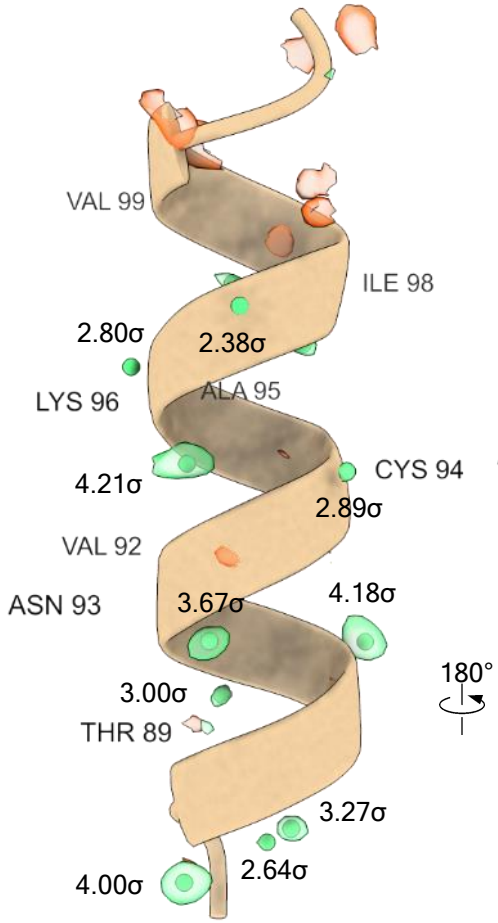

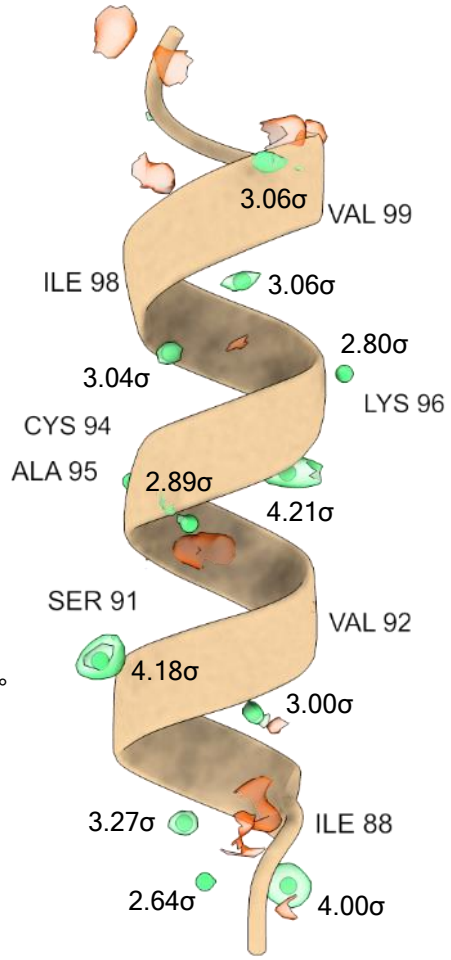

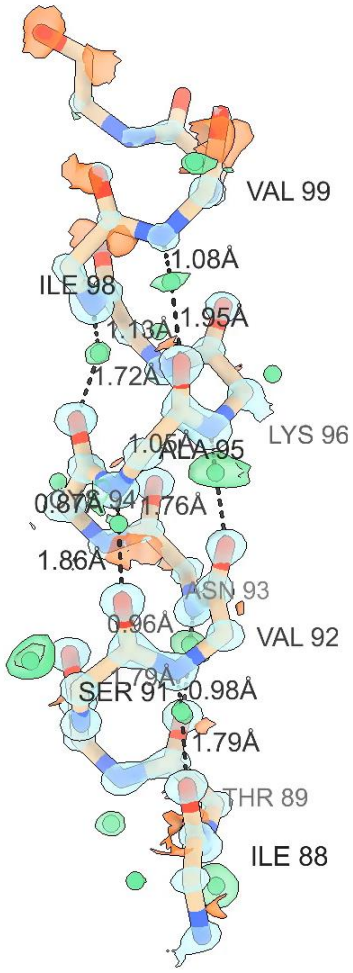

Hydrogen atoms, protonation, and hydrogen bond networks

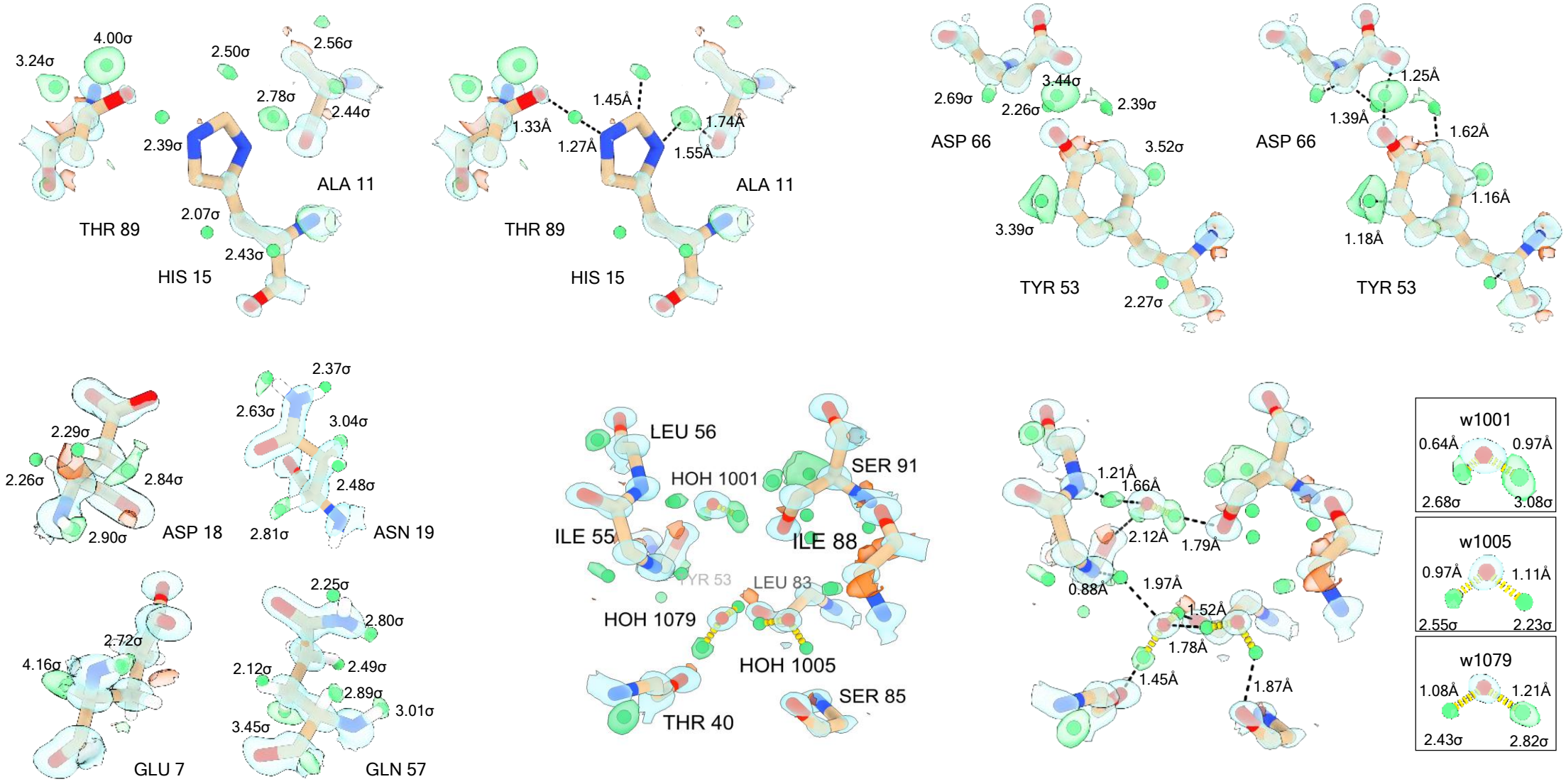

Multi-pass data collection on crystalline lamellae of proteinase K

High resolution pass

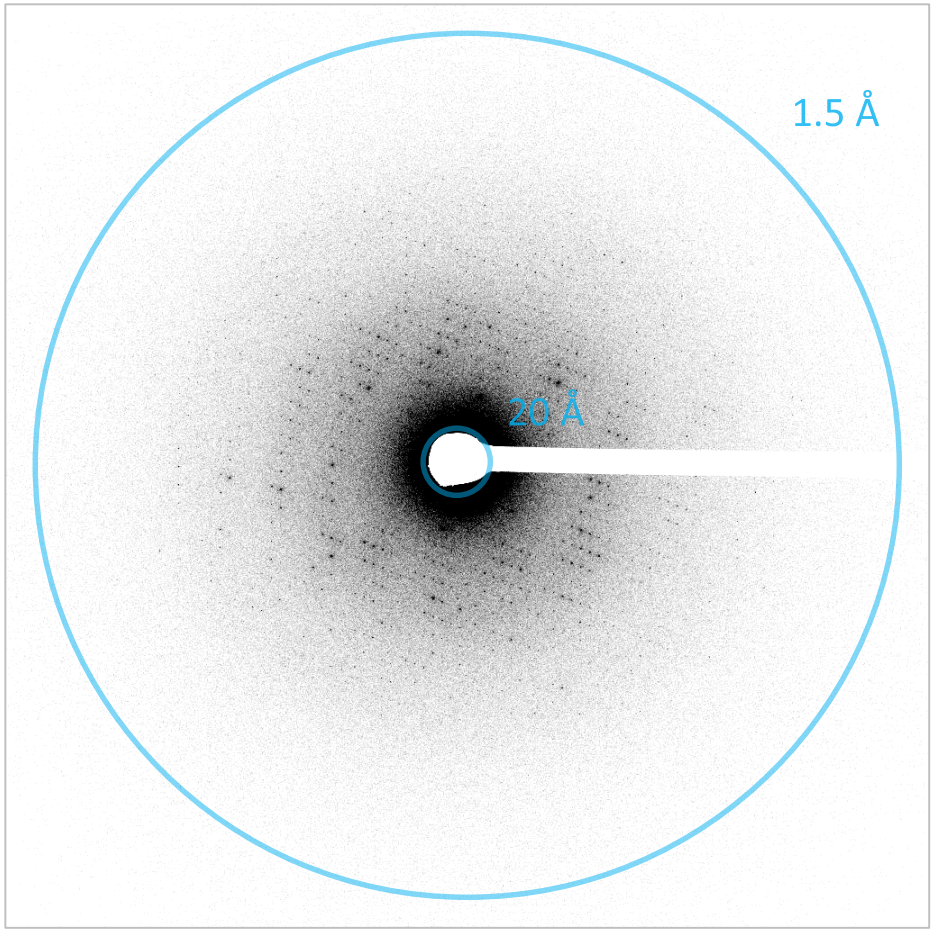

Low resolution pass

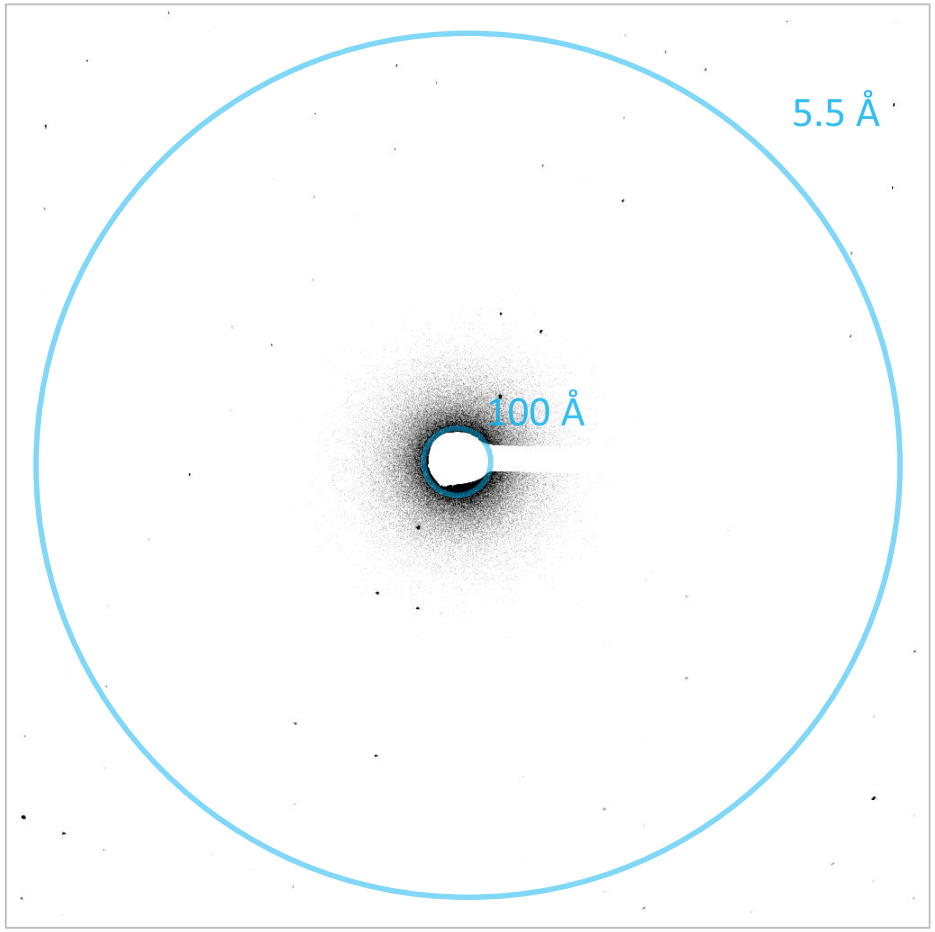

Data integration and merging of two crystal lamellae to 1.5 Å resolution

No. of crystals	2
Space group	$P4_32_12$
Unit cell dimensions	
a, *b*, *c* (Å)	67.08, 67.08, 106.78
α, *β*, *γ* (°)	90, 90, 90
Resolution (Å)	43.35-1.50 (1.55-1.50)
Observed reflections	416133 (36794)
Unique reflections	39347 (3683)
Multiplicity	10.6 (9.9)
Completeness (%)	98.87 (94.41)
R_{merge}	0.277 (1.508)
R_{meas}	0.291 (1.590)
R_{pim}	0.087 (0.492)
<I/σI>	5.65 (1.12)
$CC_{1/2}$	0.989 (0.310)

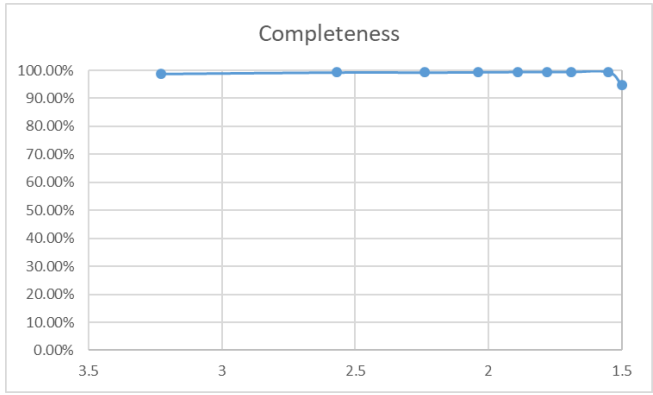

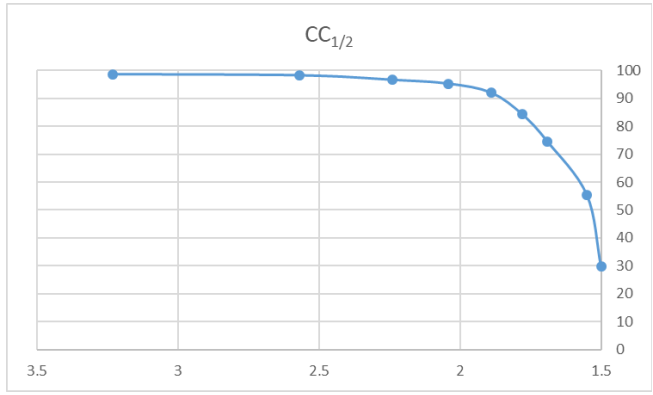

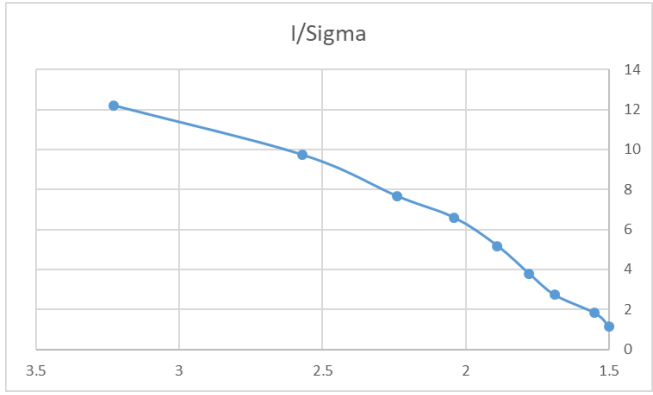

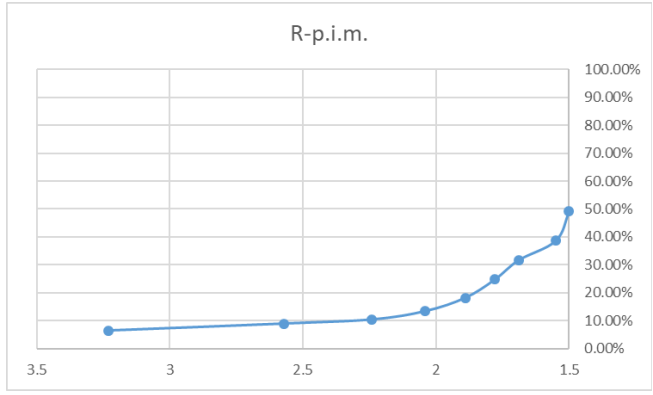

Ab initio structure determination of proteinase K at 1.5 Å resolution

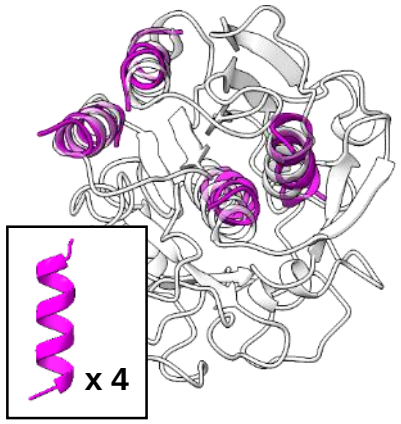

Placing fragments

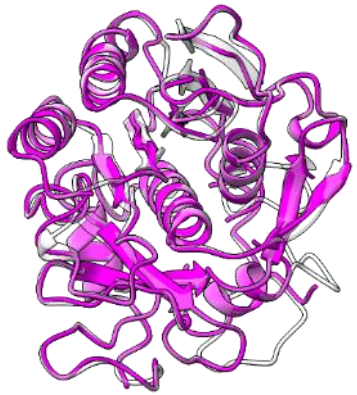

Chain tracing and density modification in *SHELXE*

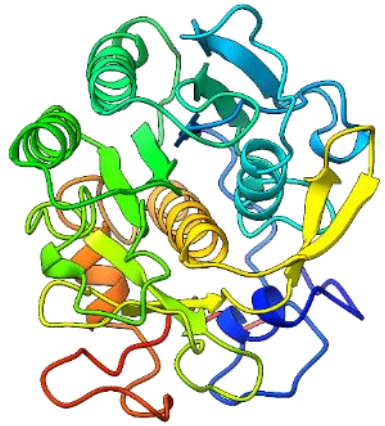

Automated model building using *BUCCANEER/REFMAC5*

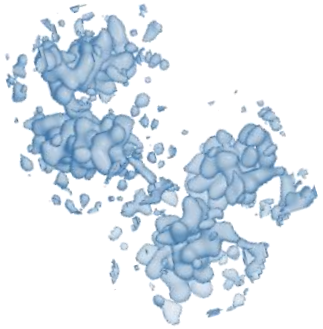

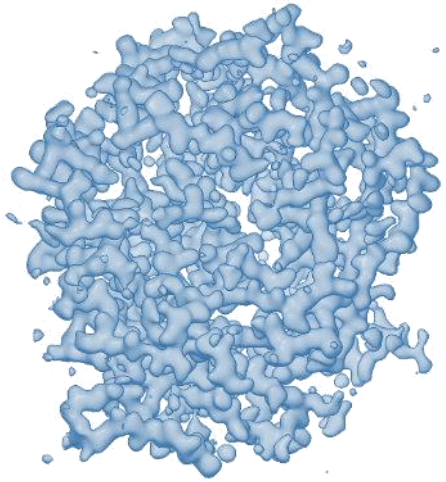

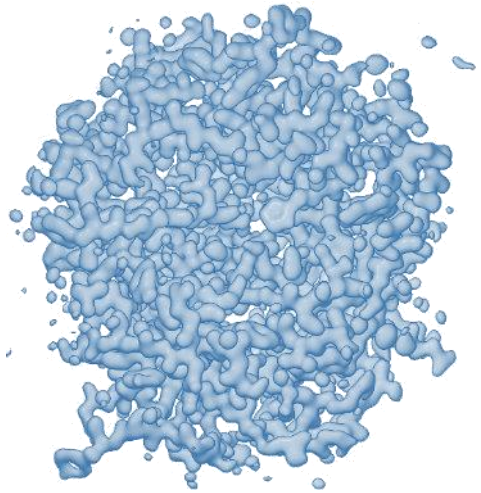

Ab initio protein structure determination using electron-counted MicroED data

Placing idealized fragments

Phase improvement

Model building and refinement

Triclinic lysozyme at 0.87 Å

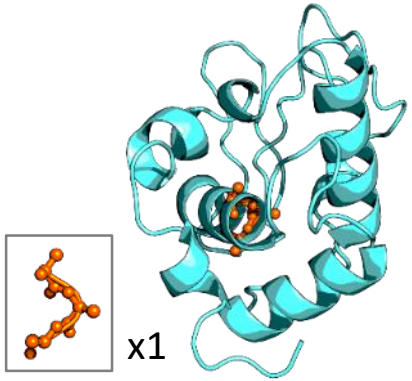

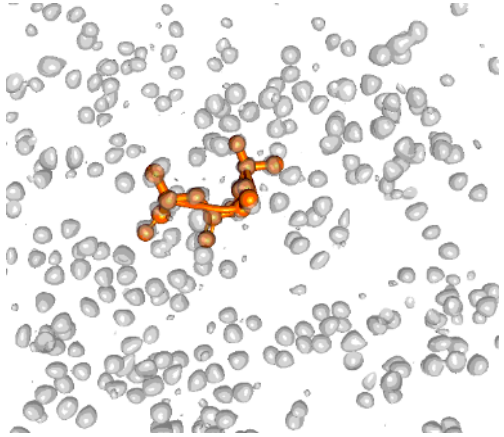

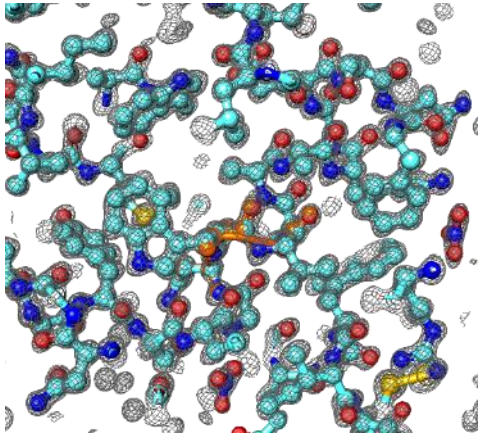

Proteinase K at 1.5 Å

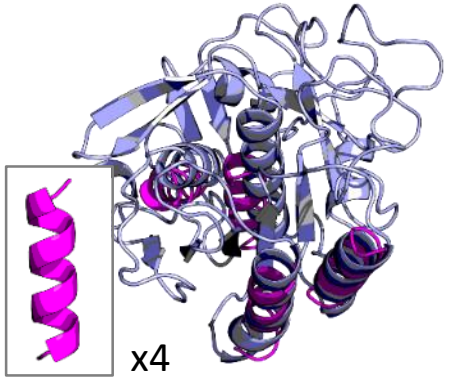

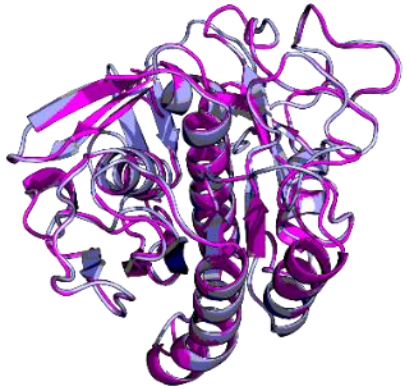

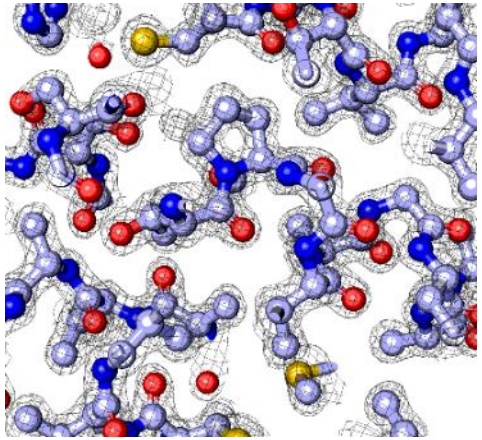

PHASER

ACORN, SHELXE

BUCCANEER, REFMAC5

Electron-counting data collection using the K3 direct electron detector

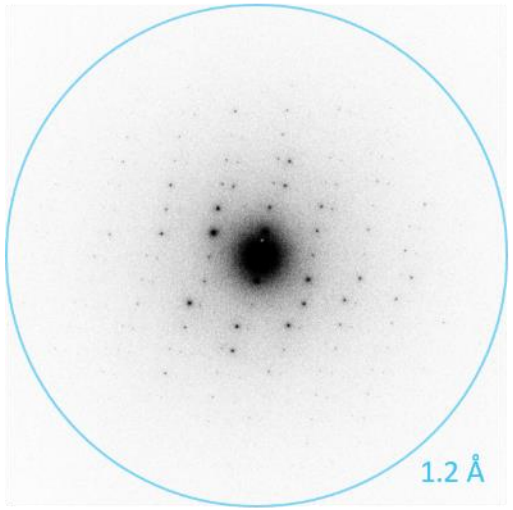

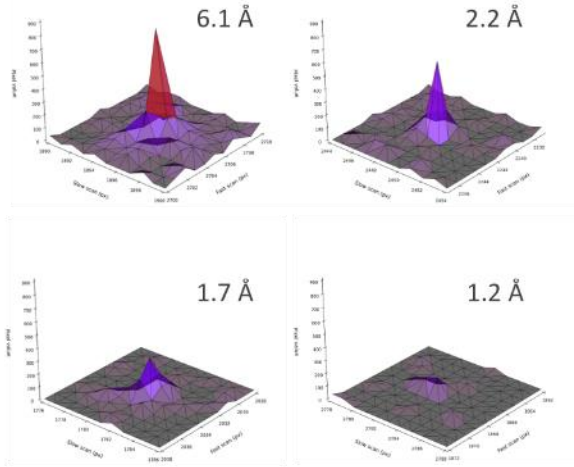

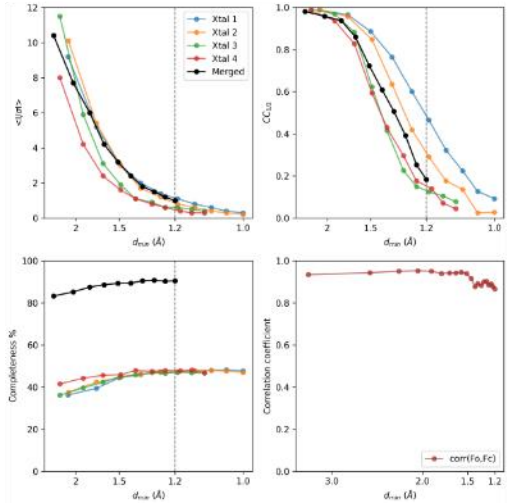

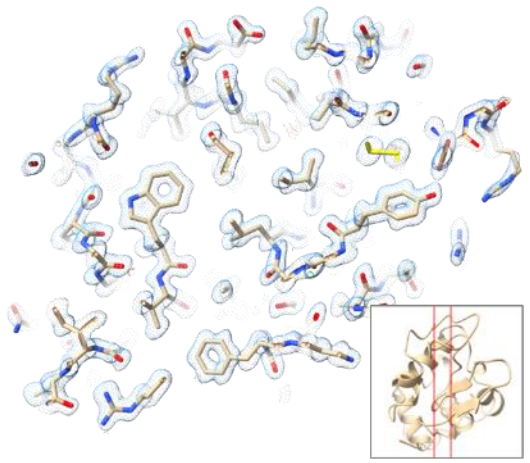

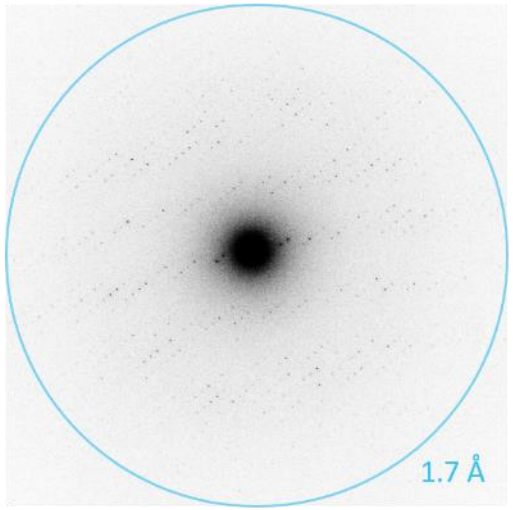

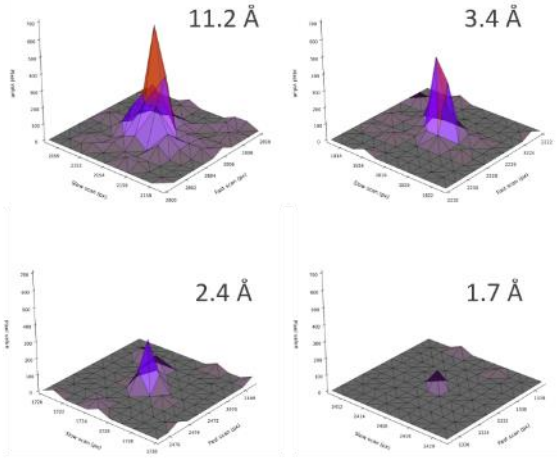

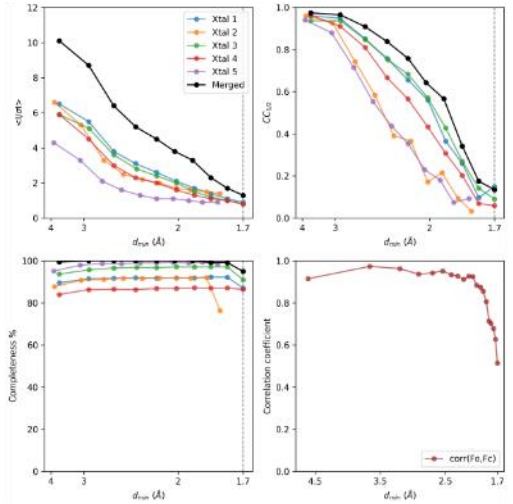

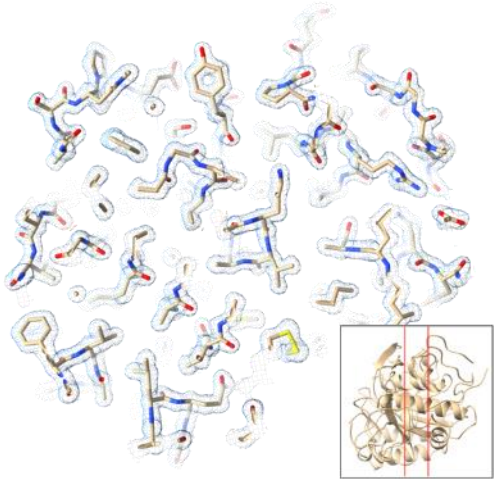

Triclinic lysozyme

Proteinase K

Routine structure determination of organic compounds using electron diffraction

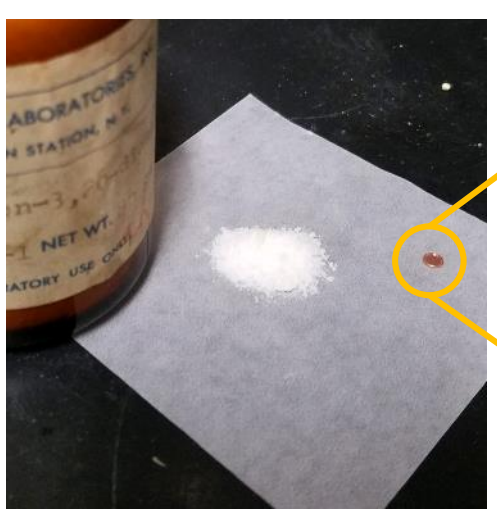

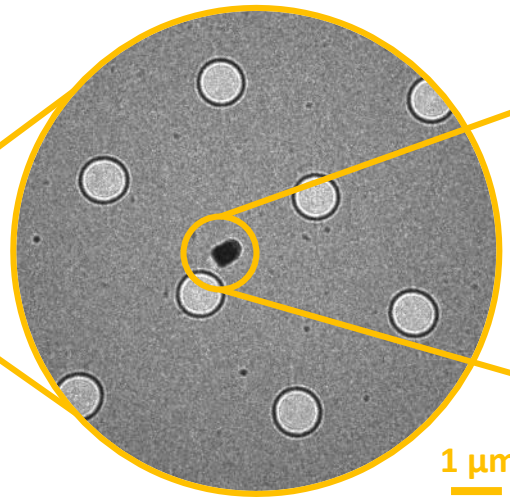

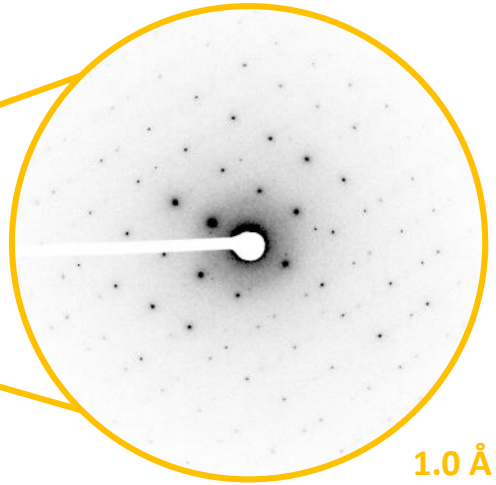

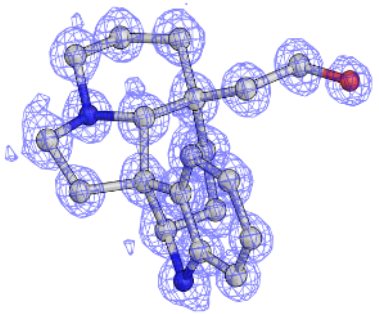

2Fo-Fc

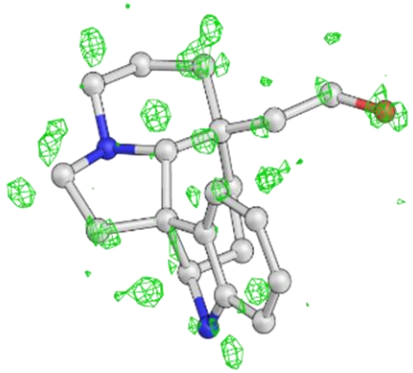

Fo-Fc

(+)-limaspermadine

Powder (~10^{-1} g) → Crystals (~10^{-15} g) → MicroED (< 3min) → Structure determination (~10min)

Gruene *et al., Ang. Chem. Int. Ed.* 57, 16313-16317 (2018); Jones *et al., ACS Cent. Sci.* 4, 1587-1592 (2018)

Identifying individual compounds from heterogenous mixtures

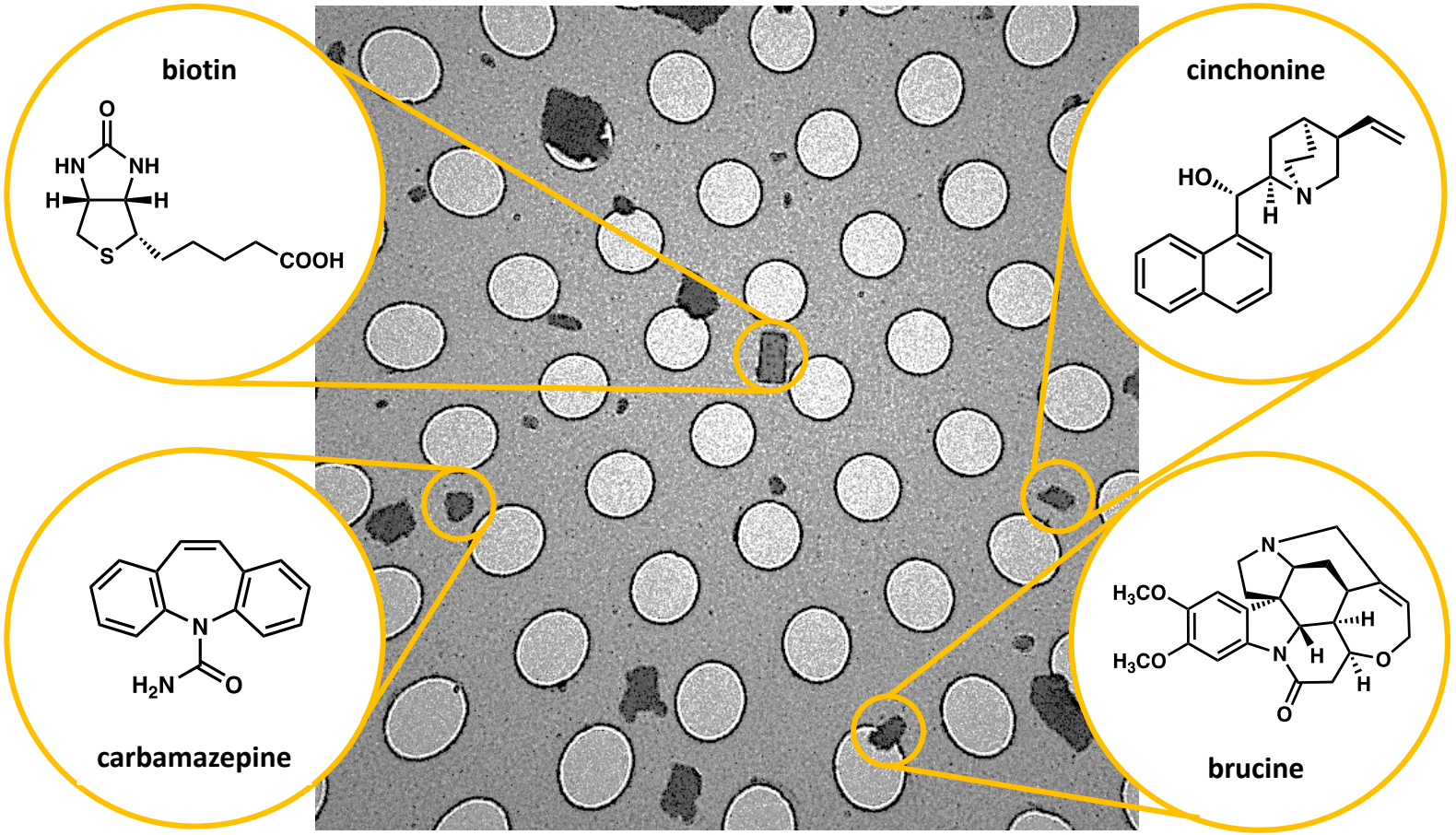

Jones *et al., ACS Cent. Sci.* 4, 1587-1592 (2018)

Automation and high-throughput serial electron diffraction enables phase identification

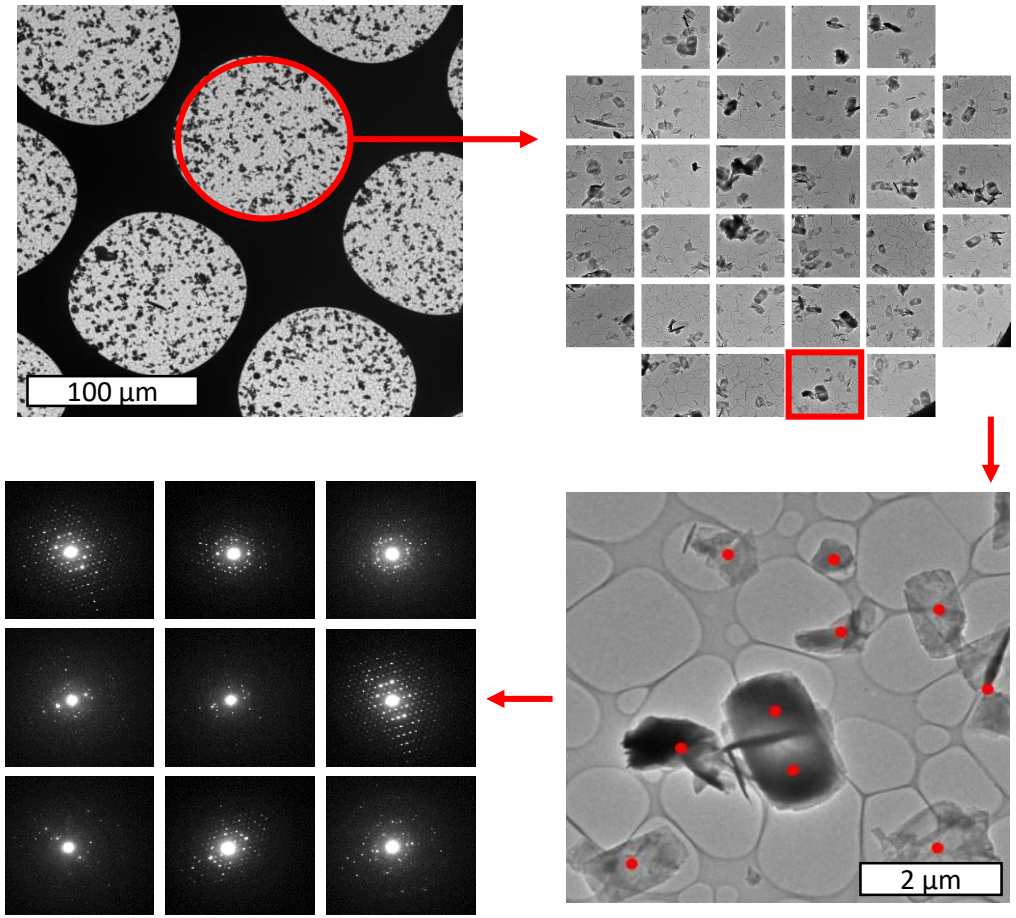

Smeets *et al.*, *J. Appl. Cryst.* 51, 1262-1273 (2017)

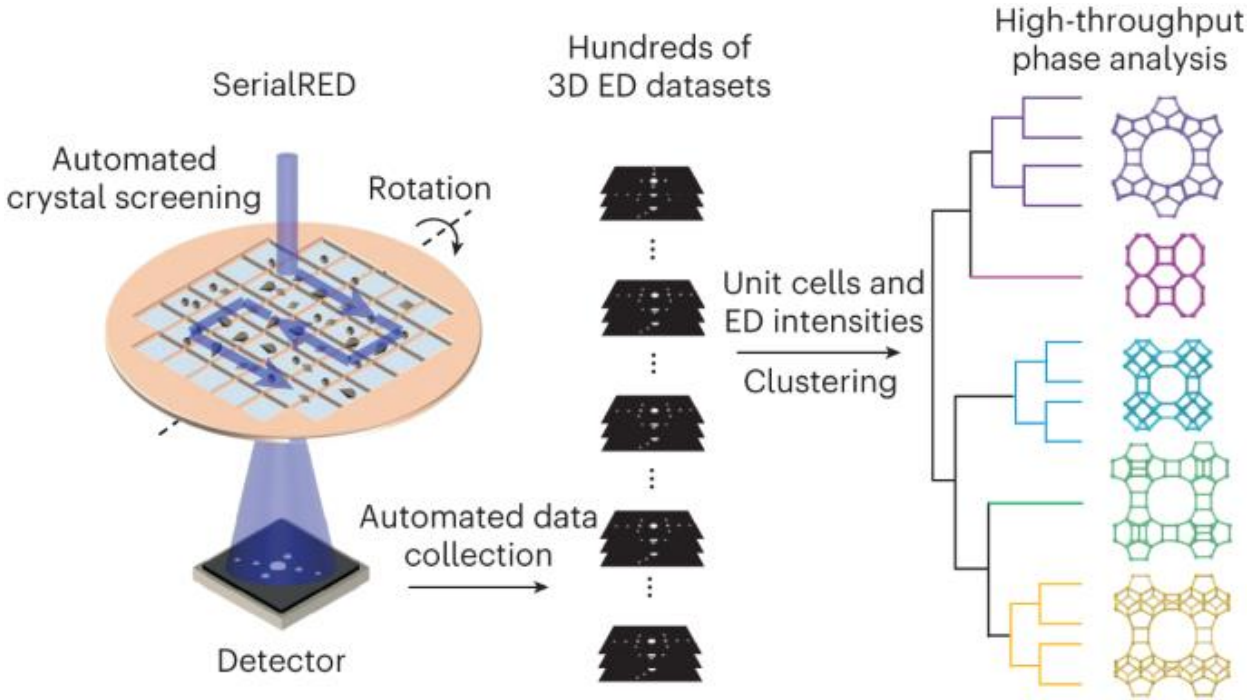

Luo *et al.*, *Nat. Chem.* 15, 483-490 (2023)

Visualizing all non-covalent interactions in nanocrystalline organic-inorganic hybrid materials

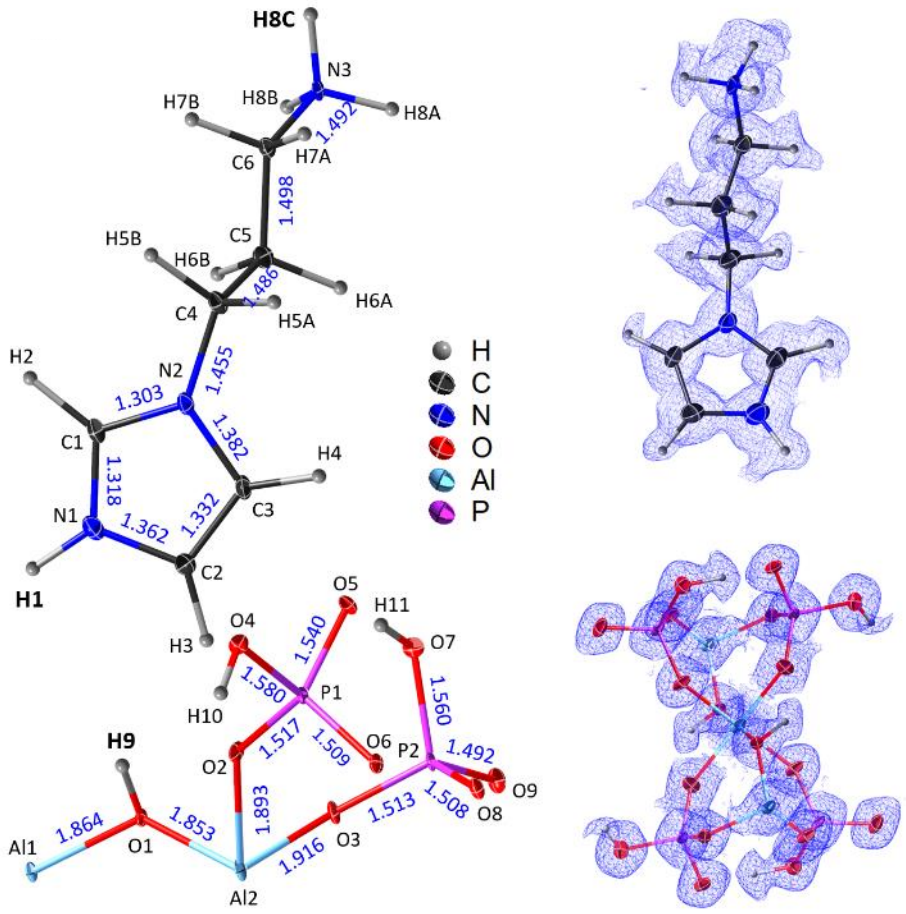

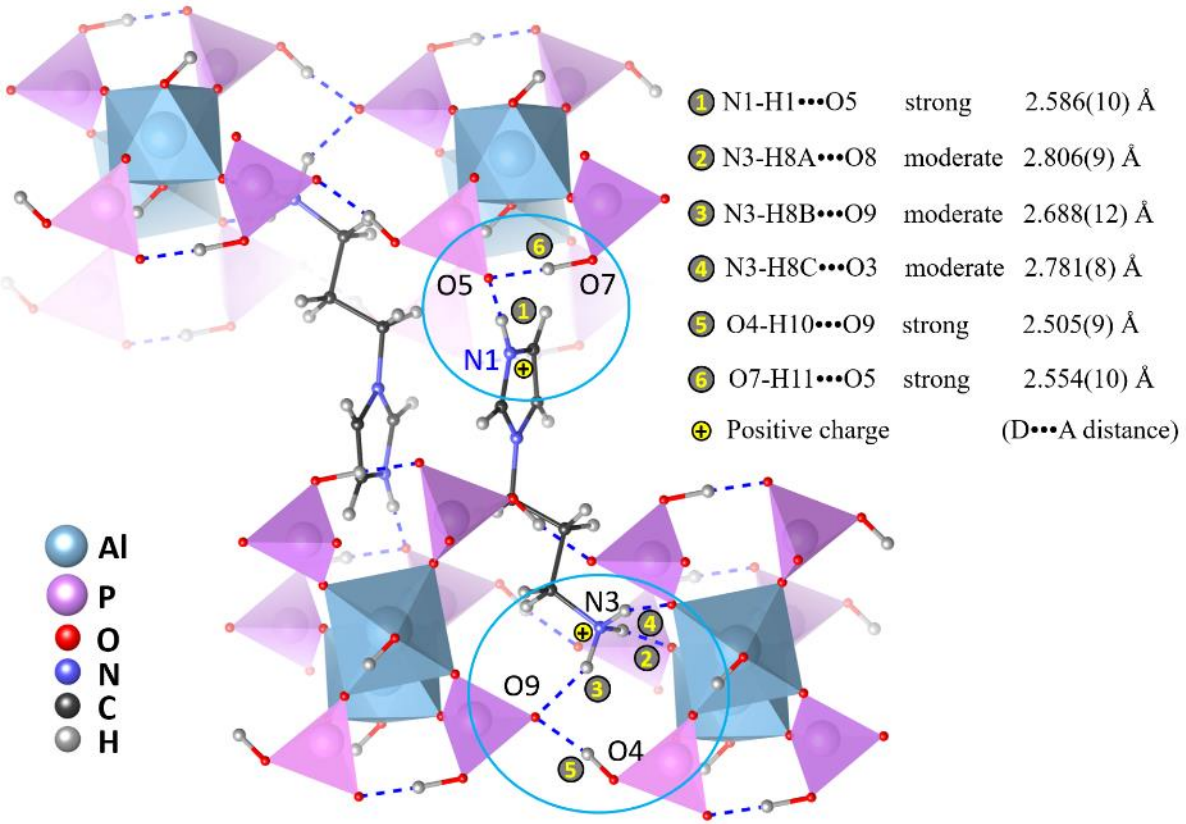

Acknowledgements

UCLA

- ❑ Tamir Gonen
- ❑ Michael Martynowycz
- ❑ Johan Hattne
- ❑ Callie Saeher
- ❑ Xuelang Mu
- ❑ Guanhong Bu
- ❑ Emma Danelius
- ❑ Marc Gallenito
- ❑ Cody Gillman
- ❑ William Nicolas
- ❑ Yasmeen Ruma
- ❑ Anna Shiriaeva
- ❑ Johan Unge
- ❑ Sara Weaver

ASU

- ❑ Brent Nannenga

Stockholm University

- ❑ Xiaodong Zou
- ❑ Sven Hovmöller
- ❑ Hongyi Xu
- ❑ Yi Luo
- ❑ Jingjing Zhao
- ❑ Martin Högbom
- ❑ Hugo Lebrette
- ❑ Mathieu Coinçon

University of Basel

- ❑ Jan Pieter Abrahams

EPFL

- ❑ Henning Stahlberg

University of Vienna

- ❑ Tim Gruene

STFC/CCP4

- ❑ David Waterman

University of Queensland

- ❑ Bostjan Kobe

Griffith University

- ❑ Thomas Ve

University of Cambridge

- ❑ Tristan Croll

Mike

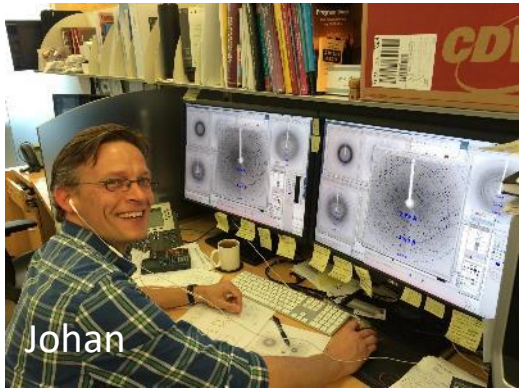

Johan

Tamir